COVID-19's U.S. Temperature Response Profile

Richard T. Carson*
Department of Economics
University of California, San Diego

Samuel L. Carson
Independent Consultant

Thayne Keegan Dye
Independent Consultant

Samuel A. Mayfield
Department of Economics
University of California, San Diego

Daniel C. Moyer
Computer Science & Artificial Intelligence Lab
Massachusetts Institute of Technology

Chu A. (Alex) Yu
Department of Economics
Wake Forest University

Revision Date: November 24, 2020

Manuscript DOI Identifier: https://doi.org/10.1101/2020.11.03.20225581

Article Summary Line: COVID-19's temperature response profile is reliably estimated using re-assembled state-reported data and suggests the onset of cold weather will amplify its spread.

Running Title: COVID-19's U.S. Temperature Response Profile

Key Words: COVID-19, data alignment, forecasting, environmental epidemiology, temperature

Abstract: We estimate the U.S. temperature response curve for COVID-19 and show transmission is highly sensitive to temperature variation despite summer outbreaks widely assumed to show otherwise. By largely replacing the daily death counts states initially reported with counts based on death certificate date, we build a week-ahead statistical forecasting model that explains most of the daily variation ($R^2 = 0.97$) and isolates COVID-19's temperature response profile ($p < 0.001$). These counts normalized at 31°C (U.S. mid-summer average) scale up to nearly 160% at 5°C. Positive cases are more temperature sensitive, scaling up to almost 400% between 31°C and 5°C. Dynamic feedback amplifies these effects, suggesting that cooling temperatures are likely to the substantially increase COVID-19 transmission.

*Address for correspondence: Professor Richard T. Carson, Department of Economics, UC San Diego, La Jolla, CA 92093, USA. Phone/Fax: (858) 534-3383/7040. Email: rcarson@ucsd.edu

Funding: The University of California, San Diego provided partial financial support for the work reported on in this paper. No outside support was received.

Competing interests: The authors declare no competing interests. Contributions to this paper by S.L. Carson and T.K. Dye were done outside of their usual employment.

Author contributions:

Richard T. Carson: Conceptualization, Methodology, Software, Validation, Formal Analysis, Investigation, Data Curation, Writing – Original Draft, Visualization, Supervision, Project Administration.
Samuel L. Carson: Investigation, Data Curation, Writing – Review and Editing.
Thayne Keegan Dye: Software, Investigation, Data Curation, Writing – Review and Editing, Visualization.
Samuel A. Mayfield: Software, Investigation, Data Curation, Writing – Review and Editing, Visualization.
Daniel C. Moyer: Methodology, Investigation, Writing – Review and Editing.
Chu A. (Alex) Yu: Methodology, Formal Analysis, Investigation, Writing – Review and Editing, Visualization.

Corresponding author biographical sketch: Dr. Richard Carson is a Distinguished Professor of Economics at UC San Diego. His research interests focus on assessing the role of climate change and other environmental variables on a range of impacts including health outcomes.

Introduction

The question of whether COVID-19 exhibits a pronounced temperature response profile has garnered attention since the early days of the pandemic *(1,2,3)*. Kissler et al.'s examination of medium and long-term management of the pandemic assigns a prominent role to understanding how the temperature response profile (hereafter "TRP") of COVID-19 might influence the pandemic's progression in the United States *(3,4)*. This follows conventional wisdom regarding the strong seasonal pattern of influenza *(5,6)*, which helped mask COVID-19's early U.S. ascent *(7)*. The recent rise in positive COVID-19 cases and related deaths across the United States has called into question whether COVID-19 transmission is adversely sensitive to summer weather. Nevertheless, some modeling groups such as the University of Washington's Institute for Health Metrics (IHME) have assumed COVID-19 activity will increase as temperatures decline and are now using information from the U.S. influenza monitoring network *(8)*, which was previously shown predictive of the pandemic's path last spring *(7)*, to help incorporate that effect.

Daily state reports often bear little resemblance to the number of COVID-19-related deaths actually occurring on that date. The resulting temporal data misalignment creates a substantial impediment to recovering any relationships with critical dependence on event timing. By reconstructing the death counts states report daily – largely by substituting in retroactive corrections based on death certificate dates – we are able to reliably estimate the TRP for COVID-19 deaths.

We assemble over 2,500 state-level daily observations from April 16–July 15, 2020, after COVID-19 became well-established across the United States. We follow the environmental economics literature on estimating pollution and temperature related impacts on a range of health and other outcomes (9). SARS-CoV-2 being a novel virus makes full implementation of the standard approach infeasible because multiple years of both spatially and temporally delineated data are not available. The specific issue we cannot currently resolve is whether the TRP over a given temperature range is the same in both directions, i.e. the cooler-to-warmer direction reflected in our data set and the warmer-to-cooler direction now occurring. It is also important to recognize that we estimate the joint, not separate, effect of any biological response by the virus and any behavioral response by the public.

Prior Efforts

Early attempts to pin down COVID-19's temperature response profile (TRP) proved it to be elusive. The now well-accepted approach for estimating influenza's TRP is epitomized by Barreca and Shimshack *(6)*, which draws heavily on the modelling of climate impacts on human populations *(9,10,11)*. Under this approach a panel data set of political entities, such as countries or their political subregions (states, counties, etc.), is assembled and the outcome of interest observed across a long time horizon (e.g., a 20-year period). The ability to employ fixed-effect indicator variables to correct for time-invariant differences between political jurisdictions, coupled with the use of short-run weather variability, provides statistical identification of a variety of impact response functions.

Prior research has three important limitations. First, cross-sectional data cannot statistically identify the desired function without making the implausible assumption that all possible confounding variables are adequately controlled for. Routinely updated time-series models slowly incorporate environmental conditions into their forecasts without ever isolating it. Short panel datasets, where the stimulus of interest has limited range (temperature, humidity, UV light, air

pollution in each location), often lack the statistical power to pin down such response functions. Consequently, estimated response functions are often fragile in the sense that statistical significance is lost when time trends or demographic variables are added to models *(12,13,14,15)*.

Second, early work (often using Chinese or cross-country data) focused on predicting speed at which the pandemic ramped up in different locations, using variants of derivative statistics like growth rates or R0*(16,17)*. These works point the 0-10°C temperature range as being most conducive to spreading COVID-19, with a possible humidity effect *(17,18,19)*. Current interest is now focused on situations where COVID-19 is spatially well-seeded and its effective R0 can move up or down with actions like state reopening plans.

Third, the quality and comparability of reported COVID-19 statistics is often suspect, particularly from the early phase of the pandemic. We move past this period to an observational window where reporting largely stabilized. A different problem now dominates temporal mismatches between when an event (e.g., a COVID-19-related death) was reported and the weather variables potentially influencing that event *(11)*. When reported event dates significantly differ from actual event dates, the resulting measurement error can overwhelm standard sources of biological variation such as individual differences in incubation periods.

Correcting State-Level COVID-19 Statistics And Why It Matters

Our ability to isolate the TRP for COVID-19 related deaths stems largely from our reconstruction of state-level COVID-19 data. The most important of these is replacing the daily death counts initially reported by states with the revised daily counts based on actual death certificate date where possible. If death certificate data is not available, we use the retroactively corrected data series that several states have produced. When available, this type of data generally rectifies many initial reporting errors. We also correct other implausible data reports such as implicit negative daily death counts and zero counts on one day followed by a clear double-count the following day. The Appendix Data Preparation section provides details.

Figure 1 displays why repairing daily state-level COVID-19 death counts matters. Panel (A) shows the originally reported (COVID Tracking Project [CTP]) CTPDailyDead_{it} daily death counts for (Florida) in blue with the "Revised" death counts by death certificate date overlaid in red. Revised curves follow the general shape predicted by epidemic models, whereas curves based on the originally reported counts have clear day-of-the-week patterns and large spikes, neither of which are predicted by biological models. Panel (B) shows the two implications. First, the confidence interval from fitting a simple quadratic trend model is dramatically larger for the CTPDailyDead_{it} (i.e., the Reported data) than the same model fit using the Revised. Second, the model based on the CTPDailyDead_{it} is slow to pick up the sharp rise in Florida deaths because the originally reported counts temporally lag the revised counts. Figure 1, Panels (C) and (D) display results for Georgia which show how use of CTPDailyDead_{it} can lead to both missing a downturn and an upturn, while supporting an incorrect story of slow progress. Appendix Figure A1 provides similar graphs for Arizona and Texas.

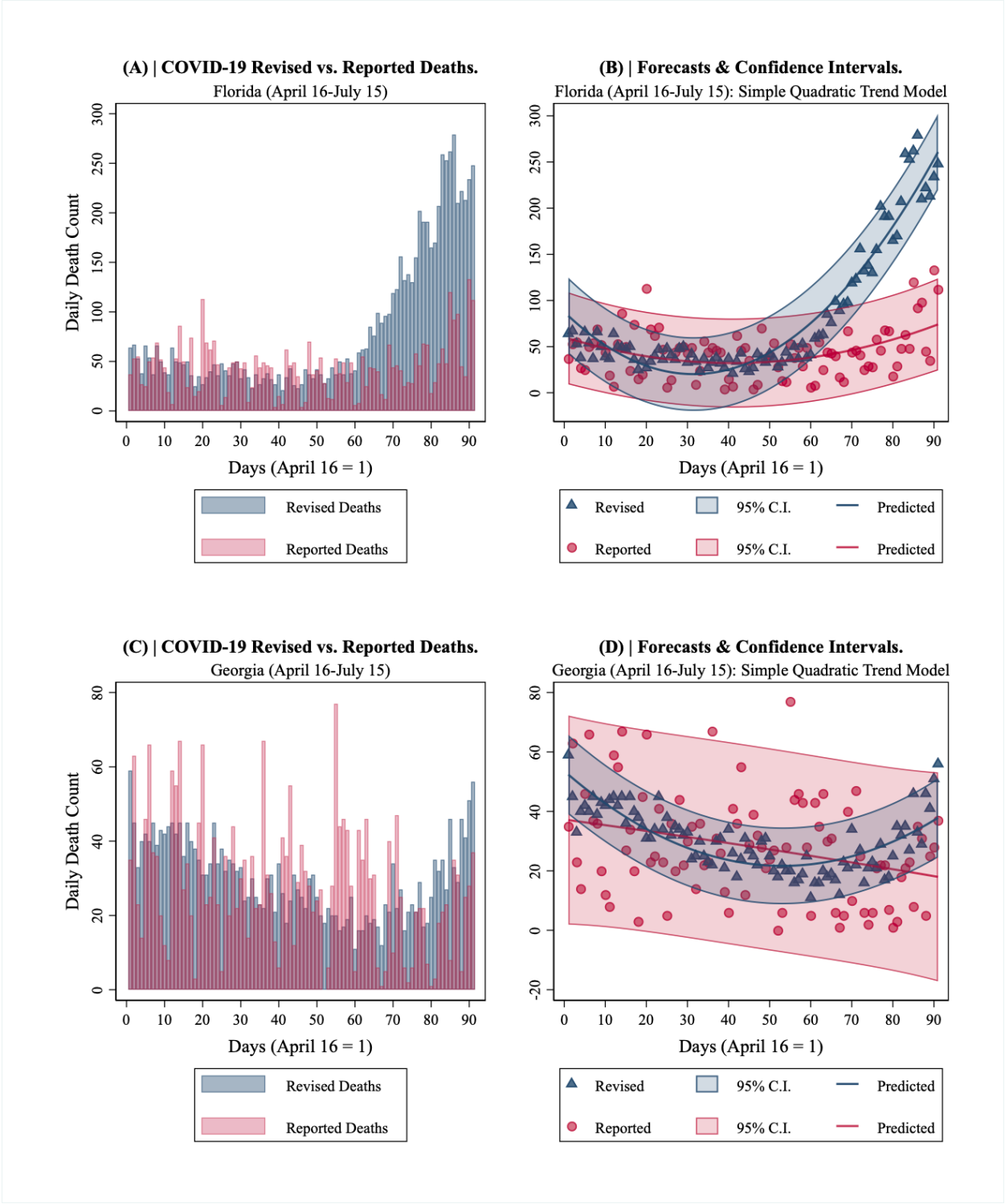

Figure 1. COVID-19 Deaths in Florida and Georgia. April 16-July 15. **(A)** Florida Revised vs. Reported. **(B)** Florida quadratic time trend forecasts and confidence intervals. **(C)** Georgia Revised vs. Reported. **(D)** Georgia quadratic time trend forecasts and confidence intervals.

Figure 2(A) shows the week ahead forecast from the University of Washington's Institute of Health Metrics and Evaluation (UW-IHME) plotted against our model's $DailyDead_{it}$ at the state

level for the entire United States over the three-month period we examine. This model explains a reasonable amount of the variance, reflected in the R^2 of .66 obtained by regressing the Revised on their forecasts. Substituting in the week-ahead forecasts from one of the other heavily used forecasting models results in a similar overall impression.

Figure 2(B) plots the predicted DailyDead_{it} using Eq. 1, which only uses information available a week earlier. This regression's R^2 of .97 is reflected in the very tight scatter plot. Since our model is relatively simple, the main source of the improvement in the percent of the variance explained is building the model off the temporally-aligned death counts provided by states post-hoc.

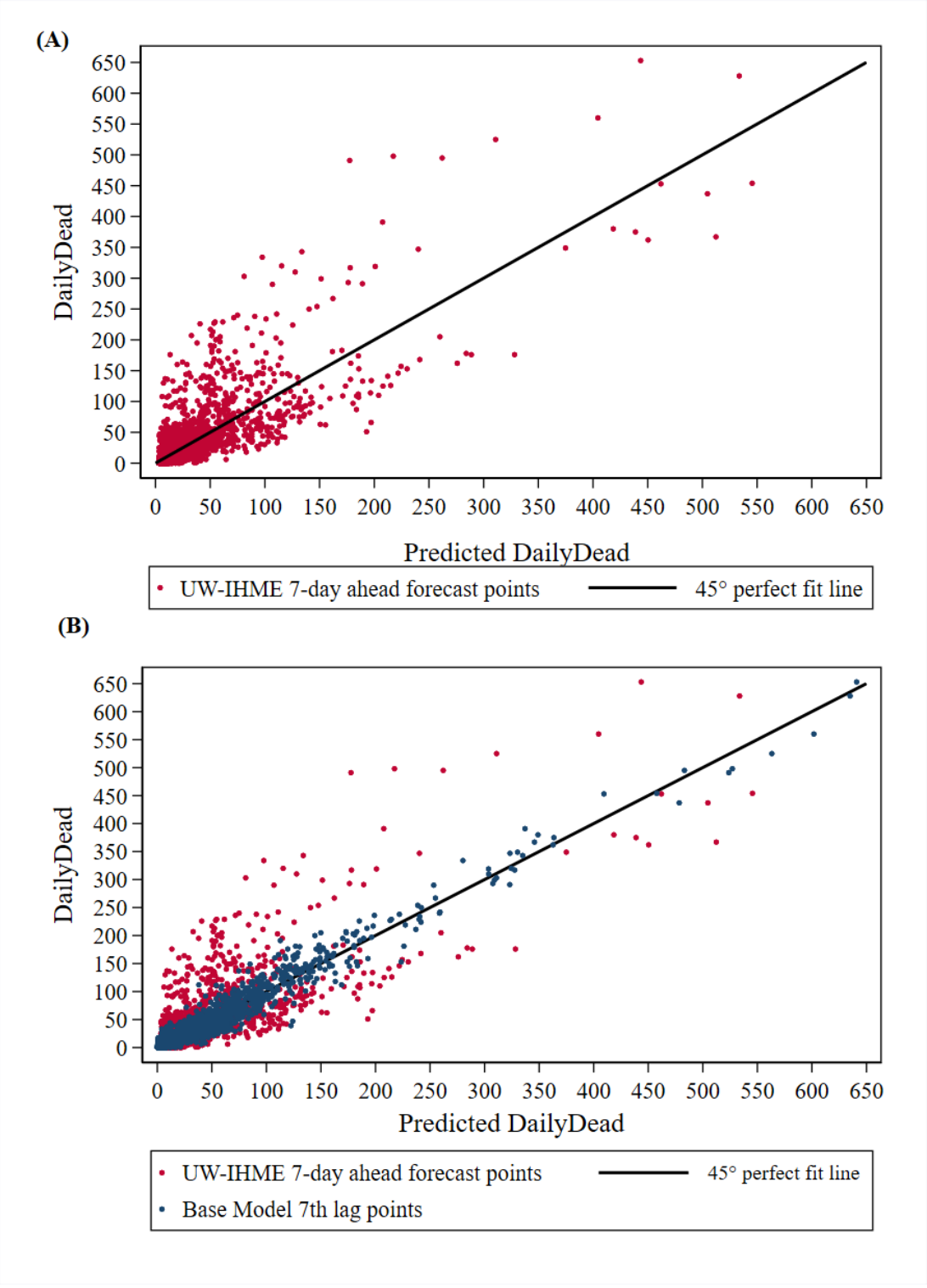

Figure 2. DailyDead$_{it}$ vs. predicted values using information available 7 days earlier. U.S. States April 16-July 15. **(A)** UW-IHME forecasts (R^2 = .66). **(B)** Eq. 1 base model predictions (R^2 = .97).

Modelling Approach

Our objective is to isolate COVID-19's TRPs with respect to state-level daily death counts ($DailyDead_{it}$) and new positive test counts ($NewPositives_{it}$). Any TRP specification should allow for the possibility of non-responsiveness (i.e., zero temperature dependence). TRPs should not incorporate fixed factors like state demographics, nor other factors associated with calendar date or a clear temporal profile. Rather, daily exogenous variation in temperature on any specific day should be the source of statistical information for identifying the TRP of interest. Intuitively, the TRP is being statistically identified by having days where the lagged count of the COVID-statistic of interest is approximately the same magnitude but a range of different temperatures is observed. The number of such comparable days is substantially increased by the introduction of controls for conditions that remain fixed across states and a flexible time trend. Statistical modeling issues revolve around functional forms and the specification of the relevant lag structure. The slow-moving, systematic changes in temperature over time imply that, over short time horizons, temperature will not be the driving force behind $DailyDead_{it}$ and $NewPositives_{it}$. However, over longer time horizons, a virus's TRP can be a major factor.

We index $DailyDead_{it}$ and $NewPositives_{it}$ by state (i) and day (t). For each we build a simple week-ahead forecasting model, controlling for state-level fixed effects and including a quadratic time trend. We then examine how lagged (t-k) maximum daily temperature ($MaxTemp_{it-k}$) scales the model's predicted $DailyDead_{it}$ or $NewPositives_{it}$. Attention is restricted to conditions where $MaxTemp_{it} \geqslant 5^{\circ}$ C, since data below this level is sparse during our sample period and concentrated in a few sparsely populated states like Alaska and Montana. Empirical estimates of our TRPs are normalized to 100 at 31°C (~88°F) – the U.S. population-weighted average for the last week of our sample – to aid interpretability.

The pandemic modelling community has largely concentrated on $DailyDead_{it}$, believing it to be a more reliable indicator of the COVID-19 infection pool than $NewPositives_{it}$ due to the large differences in testing regimes across states and time. We proceed in a similar manner, but also produce the TRP for $NewPositives_{it}$ (conditioning on available testing information) since it is positive cases that are potentially directly influenced by temperature.

Model Components

Our base $DailyDead_{it}$ statistical model (Eq. 1) is comprised of two multiplicative components. The first produces expected current-period deaths as a function of past observed deaths at a fixed temperature. The second allows expected $DailyDead_{it}$ to (potentially) vary with past values of $MaxTemp_{it-k}$.

The terms inside the first component are the infection pool proxy, $DailyDead_{it-7,}$ state-level fixed effect indicators, $StateIndicator_i$ and a quadratic time trend in $Days_t$ (t=1, …, 137; initialized to March 1 to aid interpretability). The $StateIndicator_i$ captures the influence of a wide range of variables which remain constant over the period examined, such as demographic composition, geographic links between locales that influence infections, and public health infrastructure. The time trend variables pick up the decline in the case fatality rate and the average effect over time of initial lockdowns, social distancing, and state re-openings. The first component is exponentiated to incorporate the restriction that expected $DailyDead_{it}$ should not be negative if COVID-19 transmission is active anywhere in the set of connected units examined. Commensurately, we use

$LogDailyDead_{it-k}$ and $LogDays_t$ as regressors, so this component can be interpreted as a log-log regression model with state-level fixed effects.

The second component is a logistic function scaling predicted $DailyDead_{it}$ up or down with $MaxTemp_{it-k}$. Deaths on specific days are the result of infections propagated over earlier days. We use $LogMaxTemp_{it-7}$ and $LogMaxTemp_{it-14}$ (one and two weeks in the past respectively) to roughly encompass the relevant period for temperature influencing current period deaths. Our panel data model specification uses an additive error term necessitates using nonlinear least squares to solve the model (*20,21*), but decouples conditional mean estimates from the estimated error component.

Formally, our base model for U.S. state *i* on day *t* is given by:

$$DailyDead_{it} = EXP(\Sigma_i\, StateIndicator_i + \alpha_1 LogDays_t + \alpha_2 LogDays_t^2 + \beta LogDailyDead_{it-7}) \\ X\ (1/(1 + EXP(LogMaxTemp_{it-7})^{\Upsilon 1}))*(1/(1 + EXP(LogMaxTemp_{it-14})^{\Upsilon 2})) \\ + \varepsilon_{it}, \qquad (1)$$

where estimated coefficients for the $StateIndicator_i$, and the Greek letter parameters minimize the sum of the squared error term of the estimated ε_{it}. The $NewPositives_{it}$ model is similarly structured.

We investigate (Appendix Table A6) the sensitivity of our results to a range of alternative specifications (e.g., different infection pool indicators, different temperature scaling functions, adding absolute humidity, relative humidity, ultraviolet radiation, inclusion of shelter-in-place/reopening orders, lagged cumulative death counts, and use of the CTP death counts) and provide further discussion of modelling issues in the Appendix Modeling Approach section.

Data

Our analysis uses three main types of data:

1. COVID-19 statistics for state-level death counts, positive cases, and tests, using The COVID Tracking Project (CTP; covidtracking.com) as our base information source.
2. Temperature data from the U.S. National Weather Service Integrated Surface Database.
3. State-level indicators and time variables.

We undertook extensive repair of the COVID-19 data reported daily by states, particularly those involving death counts. A dominant feature of these data are the substantial lags between when many of these events officially occurred and when they are reported. It is not uncommon to see states include deaths from several weeks prior in any given day's count.

Over half of the U.S. states have made the number of COVID-related deaths publicly available by their death certificate dates in some manner (Appendix, Data Preparation). A simple OLS regression of death counts by death certificate date on originally reported death counts for many of these states yields an R^2 of less than 0.5. Other states have made corrections to originally reported COVID-19 statistics. These updated counts tend to retroactively correct a myriad of reporting errors by states contained in the CTP daily data snapshot. These issues include failing to report any information on specific days, decisions on "probable" COVID-related deaths, and the resolution of duplicated death certificates. We use states' self-corrected counts when available.

When neither of these two sources of information was available, we undertook a consistent set of data repair operations. These include: averaging across days with no reporting, prorating backwards in time large batches of deaths (and other statistics) known to have occurred over a much longer period (typically from nursing homes), and making the minimum set of changes

necessary to correct logical violations such as negative counts of new deaths, positive cases, and tests. We make this dataset available for use by other researchers, along with a line-by-line account of the corrections made.

For each state, weather variables are taken from the airport with the highest volume of commercial traffic. We focus on maximum daily temperature. Mean temperature results are quite similar. State-level aggregation requires taking weather data from a single station. Measurement error induced by this compromise is likely to be less than one might think. Many states are small spatially or have a single, concentrated metropolitan area (e.g., Illinois). In spatially large states with large populations, most of the population often lives within reasonable proximity to the largest airport. Even in Texas, most people live along the corridor between Dallas (DFW is our representative airport) and Houston. As a result, over 60% of the American population lives within 300km of the representative airport for their state. Similarly, positive cases are also concentrated in major metropolitan areas near those airports. More generally, a single source of classical measurement error attenuates parameter estimates toward finding no effect.

Daily Dead Model Results

Eq. 1 is estimated using non-linear least squares and has an R^2 of 0.97. All parameter estimates (provided in Appendix Table A1) using robust standard errors clustered at the state-level are significant. Figure 2(B) displays the Revised $DailyDead_{it}$ versus the model's in-sample predicted values. States where the actual death certificate dates were available have considerably smaller prediction errors (Model 2 in Appendix Table A6).

The model's quadratic time trend suggests $DailyDead_{it}$ has fallen over time; at a declining rate from mid-April through the end of May, and then almost flat (slowly rising). $LogDailyDead_{it-7}$ is the dominant predictor and its coefficient estimate of 0.8686 (t=35.32) has a standard elasticity interpretation.

Figure 3 shows the estimated TRP implied by the parameter estimates for the two $MaxTemp_{it}$ lags in the logistic scaling function. The vertical axis represents expected $DailyDead_{it}$ at each temperature value when both lags are set to the same temperature and the TRP is normalized to 100 at 31°C. (Appendix Figure A9 show the corresponding TRP using the original CTP death counts.) Appendix Figure A2 provides the contour plot which allows the two $MaxTemp_{it-k}$ lags values to vary independently.

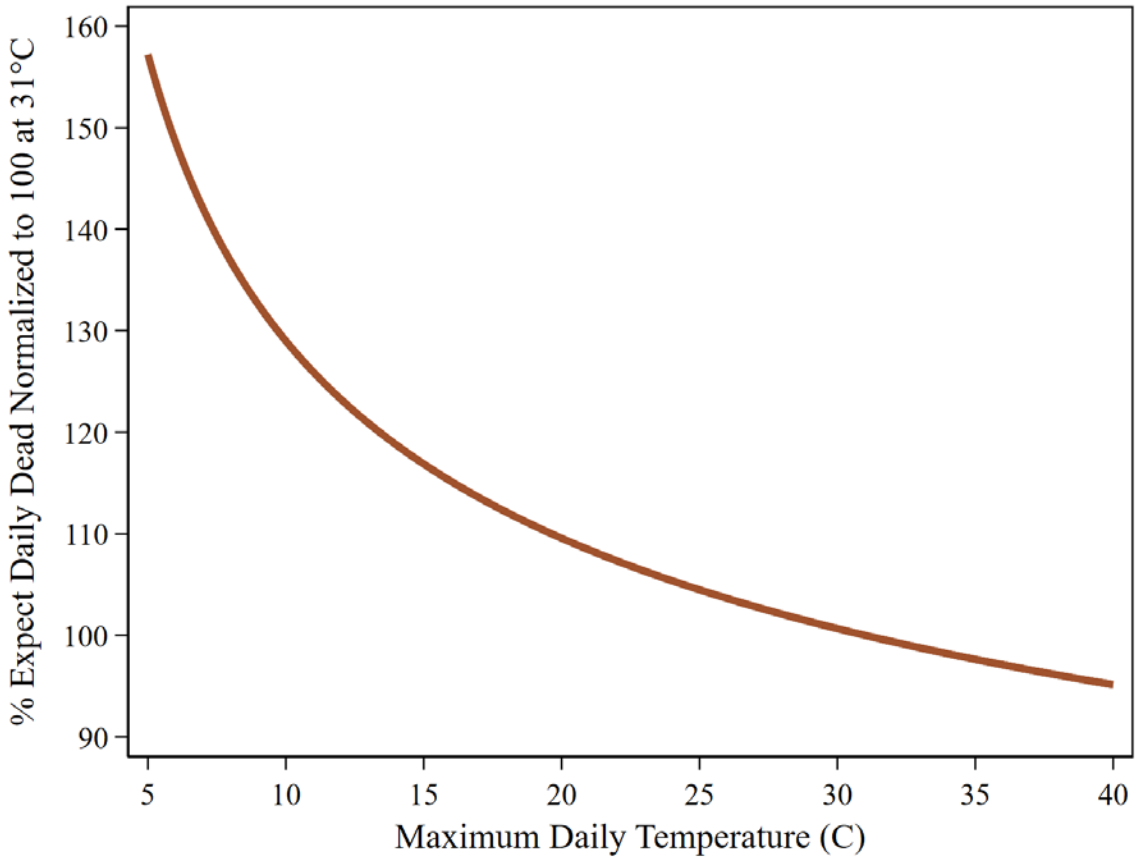

Figure 3. COVID-19 daily dead temperature response profile. U.S. states: April 16-July 15. Temperatures for 7th & 14th lags set equal.

Differentiating Eq. 1 with respect to $DailyDead_{it-7}$ produces a measure of how the expected $DailyDead_{it}$ increases from a one death increase in $DailyDead_{it-7}$. Setting *t* and $MaxTemp_{it-k}$ to chosen values yields $[TRP*\beta*EXP(StateBase_{it})]/(DailyDead_{it-7})^{(1-\beta)}$, where the TRP directly scales the elasticity parameter, β, on $LogDailyDead_{it-7}$, and $StateBase_{it}$ is the temporally varying sum of the fixed $StateIndicator_i$ and the quadratic time trend. As an example, for Georgia on July 15 ($StateBase_{it}$ = 3.9184, $MaxTemp_{it-7}$ = 29.4, $MaxTemp_{it-14}$ = 27.8 and the corresponding non-normalized TRP = 0.0368), changing $DailyDead_{it-7}$ from 27 to 28 is predicted to increase the expected $DailyDead_{it}$ by 1.0457. Appendix Figure A3(B) displays a variant of this calculation for individual states as $DailyDead_{it-7}$ increases from 0 to 1.

We simulate $DailyDead_{it}$ predictions from both static and dynamic variants of our estimated base model (Eq 1) by taking $DailyDead_{it-7}$ from our sample period's last week and $MaxTemp_{it}$ = 31°C as the initial values to propagate the simulation. We fix $MaxTemp_{it-7}$ and $MaxTemp_{it-14}$ at 31°C from day 1 to day 45 to mimic the rest of the summer period, then progressively decrease them by 0.2°C each day until 5°C is hit, which occurs on day 175, after which temperature is held constant.

The brown dashed line in Figure 4 provides a stylized static [left vertical axis] representation of information contained in our base model (Eq. 1) using Georgia as an example (since it starts out at just below our 31C° normalization point and in a cold year hits our 5C° endpoint). The two $MaxTemp_{it-k}$ change in tandem, with all other variables fixed at their initial values. In this static response model expected $DailyDead_{it}$ increases through only one channel: the direct impact of lowering temperature.

The blue dashed curve in Figure 4 shows the dynamic counterpart [right vertical axis] that allows $MaxTemp_{it-k}$ to influence $DailyDead_{it}$, which is then used as the lagged model input for subsequent projections. Temperature affects expected $DailyDead_{it}$ through two channels: the direct effect shown in the static model and the indirect, compounding effect of when the initial death count of each cycle of the simulation is set to a lag of the previous output. The indirect effect of maximum temperature is the dominant mechanism, accounting for more than 90% of the increase in the expected death count as temperature falls from 31°C to 5°C. The inset in Figure 4 plots the two curves under the same scale and conveys the magnitude of the differences between the pure static and dynamic responses.

Neither model is likely to represent reality, but together may span it. Staying on the static TRP curve requires continual reductions in effective contact rates that exactly offset the increase in transmission potential, such that the current death count is always held to be equal to last week's death count. Observing the full dynamic effect would require the absence of offsetting actions by both the government and the public (such as increased social distancing and face mask adherence as COVID-19 activity quickly increased).

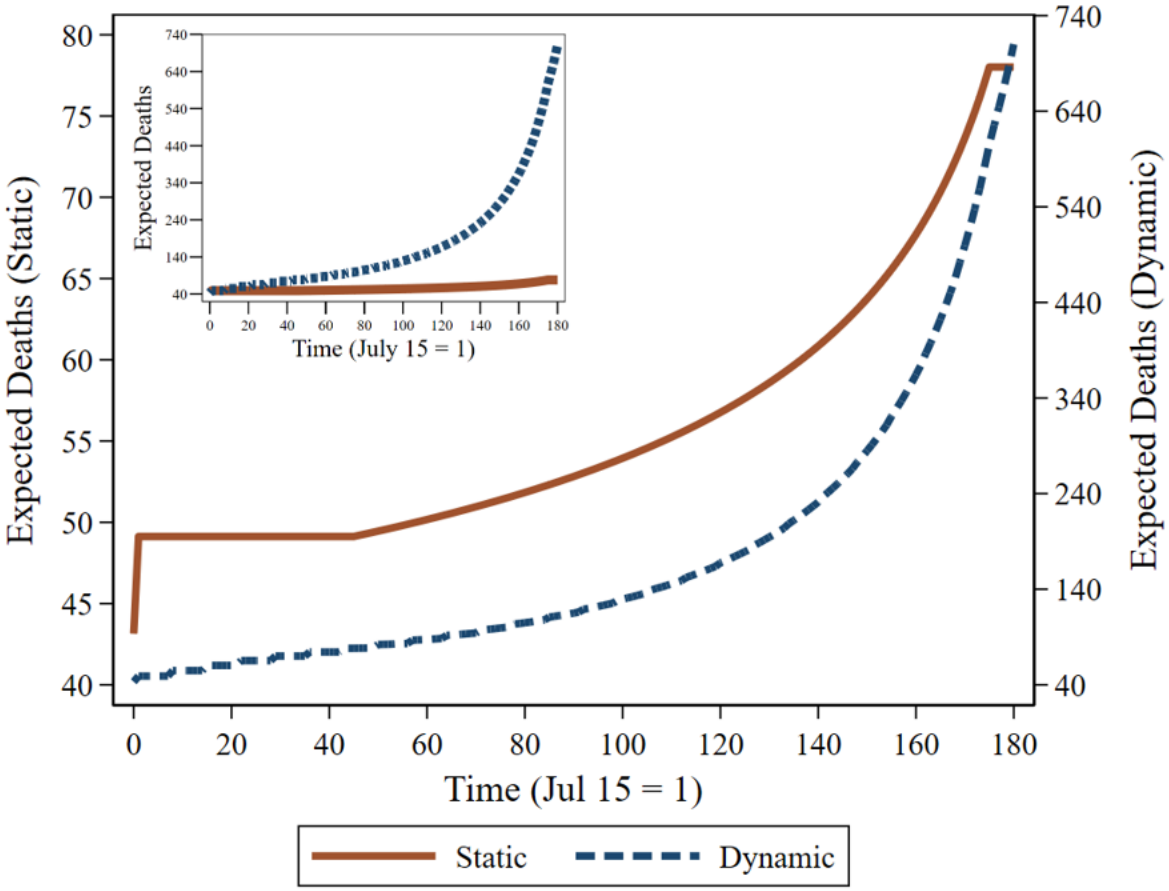

Figure 4. Stylized static and dynamic TRPs for Georgia derived from Eq. 1 parameter estimates. The brown solid curve [left vertical axis] is the stylized static TRP where temperature influences $DailyDead_{it}$ through changes to $MaxTemp_{it-k}$, with $DailyDead_{it-7}$ held constant. The blue dashed curve [right vertical axis] is stylized dynamic TRP under similar assumptions, except dynamic feedback is allowed in the form of temperature influencing subsequent $DailyDead_{it-7}$.

$StateIndicator_i$ values for some geographically isolated states with small populations like Hawaii are small enough to suggest their COVID-19 death counts would be unsustainable in warm enough weather. This is not true of most states, though, and is inconsistent with Baker et al.'s finding from examining earlier emergent viruses that warming weather is not enough by itself to stop their spread *(22)*.

The Appendix section on Alternative Specifications for Base Death Count Model describes additional analyses that (a) look at alternative temperature scaling functions, (b) substitute $DailyDead_{it-14}$ or $NewPositives_{it-7}$ for $DailyDead_{it-7}$, and (c) add the dates of state actions such as shelter-in-place orders as control variables. This work shows that our finding of a strong TRP for $DailyDead_{it}$ is quite robust. Some specifications suggest the TRP is flatter in the 10-20°C range but steeper in the 5-10°C range (Appendix Figure A8).

New Positive Case Model Results

$NewPositives_{it}$ are modeled similarly to Eq. 1, substituting $LogNewPositives_{it-7}$ as the infection pool regressor. Testing information is required to interpret reported state-level positives cases. We use $LogNewTests_{it}$, to control for current testing intensity, $LogNewTest_{it-7}$ (which allows for a past positivity rate interpretation), total tests administered per thousand lagged by one week ($PerCapitaTests_{it-7}$) to help control for prior testing intensity, and an indicator variable for systematically lower reporting on Monday. We chose $LogMaxTemp_{it-7}$ for consistency with the death count model. For the other temperature lag the 2nd lag fits best.

This model's (Appendix Table A2) R^2 is 0.95. All regressors are significant at $p < 0.001$, except for some of the test related variables: $LogNewTest_{it-7}$ (p=0.005), $PerCapitaTests_{it-7}$ (p=0.002) and Monday (p=0.015). Estimated parameters for the two lagged temperature variables are considerably larger than their $DailyDead_{it}$ counterparts. The implied TRP for $NewPositives_{it}$ is displayed in Figure 5. Appendix Figure A(4) shows contour plot allowing the two temperature lags to vary independently.

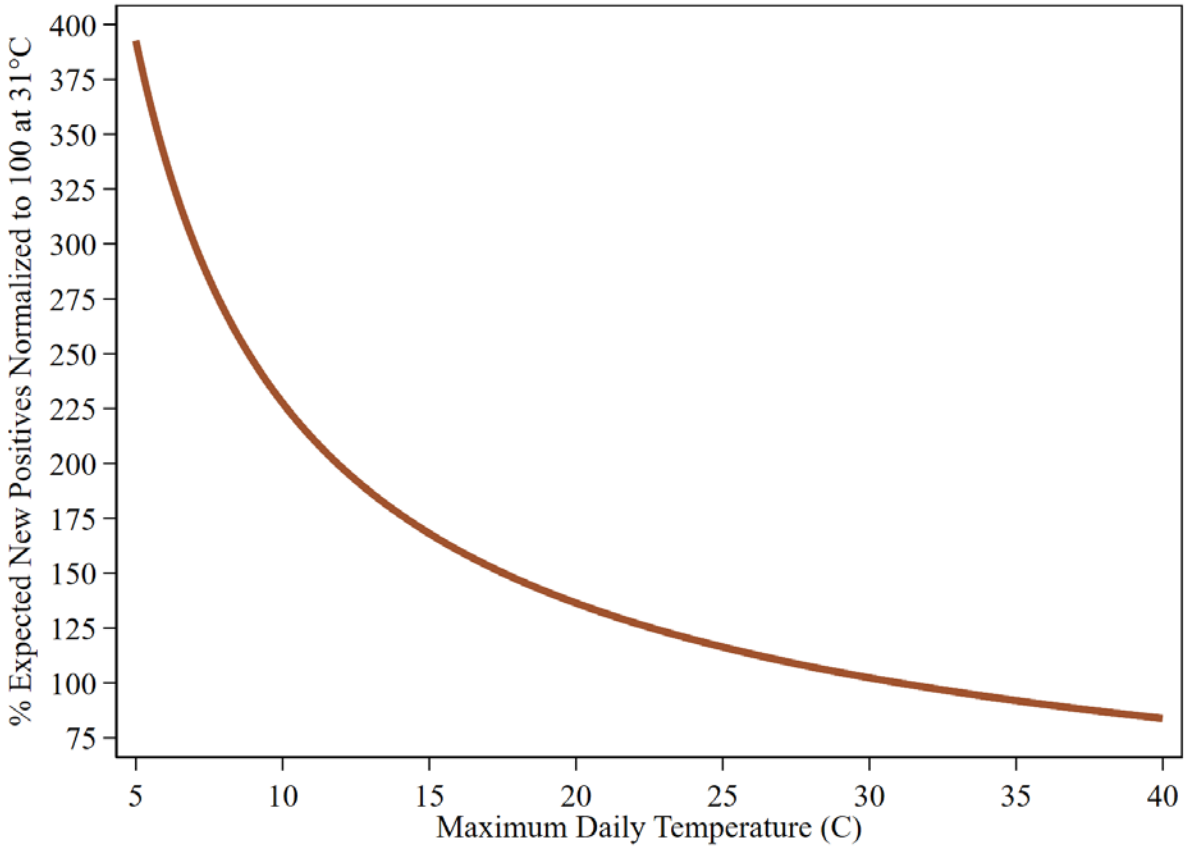

Figure 5. COVID-19: new positives temperature response profile. U.S. states: April 16-July 15. Temperatures for 2nd and 7th lags set equal.

Discussion

$DailyDead_{it}$ predictably varies with changes in maximum daily temperature (Figure 3). This relationship is considerably more pronounced for new positive cases (Figure 5). Cooler

temperatures with the progression of fall and winter will dramatically ramp up the number of new positive cases and the deaths that follow unless current infection pools are dramatically reduced. Dynamic feedback between rising infection pool indicators and cooling temperatures (Figure 4) suggests delay in responding to increased virus activity signs can result in rapid escalation. This is already being seen in the current spatial pattern of outbreaks and the ever-increasing medium-run death count forecasts (e.g., UW-IHME *(8)*). Investment in providing the pandemic modeling community with timely counts based on death certificate dates would allow them to deliver substantially more accurate and timely warnings of impending upturns.

Warming temperatures during the spring and summer actively aided efforts to reduce COVID-19's spread and may have even contributed to a false sense of the efficacy of those efforts. Cooling temperatures will present a quite different challenge. Figure 6 shows the average date over the past 30-years when each U.S. county enters the particularly dangerous 10°C to 5°C. Effects of temperature amplification show up with a lag.

There has long been fear of facing COVID-19 during influenza's October to March season *(23)*. Our results suggest, that in addition to this concern, COVID-19 transmission will become increasingly more efficient at transmission than it was during the summer. Further, if deaths and positive case TRPs behave like influenza *(6)*, both will continue to increase from 5°C until a few degrees below freezing.

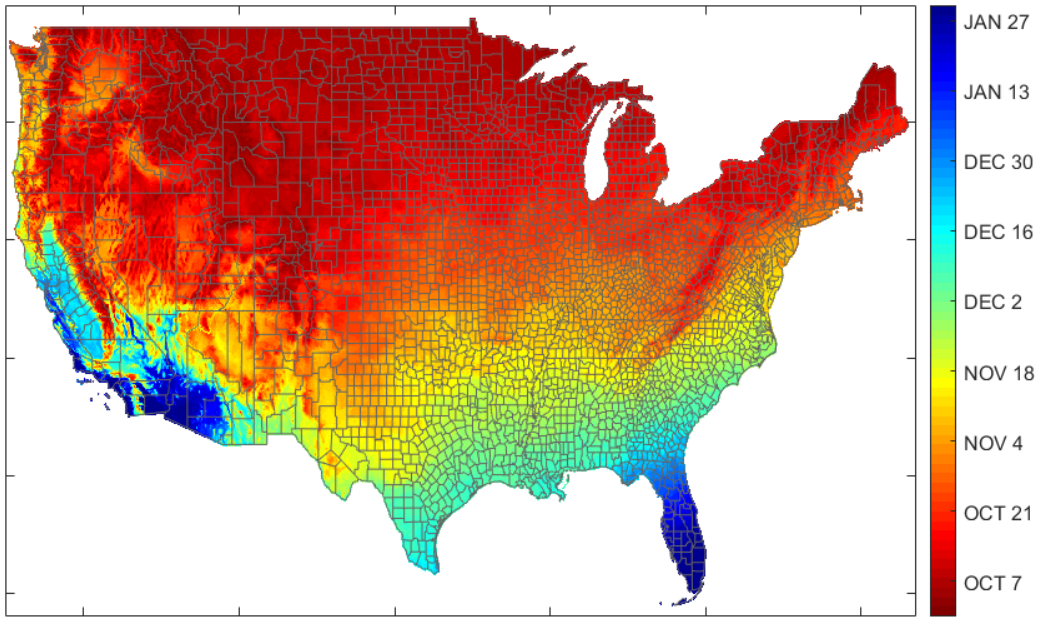

Figure 6. Expected date by U.S. county for entering 5-10°C range (30-year average).

References

1. National Academies of Sciences, Engineering, Medicine. Rapid expert consultation on SARS-CoV-2 survival in relation to temperature and humidity and potential for seasonality for the COVID-19 pandemic. 2020.

2. Kanzawa M, Spindler H, Anglemyer A, Rutherford GW. Will coronavirus disease 2019 become seasonal? J. Infect. Dis. 2020; **222**, 719-721.

3. Kissler SM, Tedijanto C, Goldstein E, Grad YH, Lipsitch M. Projecting the transmission dynamics of SARS-CoV-2 through the postpandemic period. Science. 2020; **368**, 860-868

4. Carlson CJ, Gomez AC, Bansal S, Ryan SJ. Misconceptions about weather and seasonality must not misguide COVID-19 response. Nat. Commun. 2020; **11**, 1-4.

5. Shaman J, Goldstein E, Lipsitch M. Absolute humidity and pandemic versus epidemic influenza. Am. J. Epidemiol. 2011; **173**, 127-135.

6. Barreca AI, Shimshack JP, Absolute humidity, temperature, and influenza mortality: 30 years of county-level evidence from the United States. Am. J. Epidemiol. 2012; **176**, S114-S122.

7. Silverman JD, Hupert N, Washburne AD. Using influenza surveillance networks to estimate state-specific prevalence of SARS-CoV-2 in the United States. Sci. Transl. Med. 2020; **12**.

8. Institute for Health Metrics, University of Washington, http://www.healthdata.org/news-release/ ihme-models-show-second-wave-covid-19-beginning-september-15-us

9. Graff Zivin J, Neidell M. Environment, health, and human capital. J. Econ. Lit. 2013;**51**, 689-730.

10. Auffhammer M, Hsiang SM, Schlenker W, Sobel A. Using weather data and climate model output in economic analyses of climate change. Rev. Environ. Econ. Policy. 2013; **7**, 181-198.

11. Hsiang, S. Climate econometrics. Annu. Rev. Resour. Econ. 2016; **8**, 43-75.

12. Xu R, Rahmandad H, Gupta M, DiGennaro C, Ghaffarzadegan N, Amini H, et al. The modest impact of weather and air Pollution on COVID-19 transmission. 2020; doi: http://dx.doi.org/10.2139/ssrn.3593879.

13. Briz-Redón Á, Serrano-Aroca Á. The effect of climate on the spread of the COVID-19 pandemic: A review of findings, and statistical and modelling techniques. Progress in Physical Geography: Earth and Environment. 2020; 0309133320946302.

14. Jüni P, Rothenbühler M, Bobos P, Thorpe KE, da Costa BR, Fisman DN, Slutsky AS, Gesink D. Impact of climate and public health interventions on the COVID-19 pandemic: a prospective cohort study. Can. Med. Assoc. J. 2020; **192**, E566-E573.

15. Pedrosa RHL. The dynamics of COVID-19: weather, demographics and infection timeline. 2020; doi: https://doi.org/10.1101/2020.04.21.20074450.

16. Carleton T, Cornetet J, Huybers P, Meng K, Proctor J. Evidence for Ultraviolet Radiation Decreasing COVID-19 Growth Rates: Global Estimates and Seasonal Implications. 2020; doi: http://dx.doi.org/10.2139/ssrn.3588601.

17. Wang J, Tang K, Feng K, Lv W. High Temperature and High Humidity Reduce the Transmission of COVID-19. 2020; doi: http://dx.doi.org/10.2139/ssrn.3551767.

18. Sajadi MM, Habibzadeh P, Vintzileos A, Shokouhi S, Miralles-Wilhelm F, Amoroso A. Temperature, Humidity and Latitude Analysis to Predict Potential Spread and Seasonality for COVID-19. 2020; doi: http://dx.doi.org/10.2139/ssrn.3550308.

19. Ficetola GF, Rubolini D. Climate affects global patterns of COVID-19 early outbreak dynamics. 2020; doi: https://doi.org/10.1101/2020.03.23.20040501.

20. Goldfeld SM, Quandt RE.The estimation of Cobb-Douglas type functions with multiplicative and additive errors. 1970; Int. Econ. Rev. **11**, 251-257.

21. Wooldridge JM, *Econometric analysis of cross section and panel data*. (MIT Press, Cambridge, MA, 2010).

22. Baker RE, Yang W, Vecchi GA, Metcalf CJ, Grenfell BT. Susceptible supply limits the role of climate in the early SARS-CoV-2 pandemic. Science. 2020; **369**, 315-319.

23. U.S. Centers of Disease Control and Prevention. When is flu season? https://www.cdc.gov/flu/about/season/flu-season.htm, retrieved 30 May 2020.

Appendix For

COVID-19's U.S. Temperature Response Profile

Includes:

Data Preparation

The data set used in this paper starts with the COVID-19 statistics reported by individual states as aggregated daily by The COVID Tracking Project (covidtracking.com). In preliminary work, we (and other modelling groups) found there was no plausible epidemiological model that would produce the wild up-and-down jumps in the state-level COVID-19 statistics reported daily. As a result, there is a major fork in the path of any modeling effort. Do you build a predictive model for the reported COVID-19 daily death count that policymakers see, where success is judged by minimizing the forecast error around those observable quantities? Or do you attempt to model the underlying process with an eye toward understanding key aspects of it? When the reported dependent variable systematically diverges from that being generated by the underlying process, these two approaches also fundamentally diverge. For the first path, success, to some degree, comes in uncovering the administrative procedures influencing the divergence. The second path led us to undertake a major effort to rectify and repair reported COVID-19 statistics, with a focus on recovering the temporal structure needed to provide TRP estimates.

The most important correction was replacing originally reported death counts with death counts by date of death as reflected on death certificates. Figures 1 and A1 illustrate the nature of the differences for between the original $CTPDailyDead_{it}$ and $DailyDead_{it}$ for four important states: Arizona, Florida, Georgia and Texas. The originally reported data results in substantially larger confidence intervals in predictive models and, because it lags the revised death counts, substantially reduces one's ability to detect and respond to changes in COVID-19 activity. We were able to make this correction for 26 states where deaths by death certificate information could be located. Our cutoff date of July 15 allowed for two and half months for states to make these death counts available, which should subsume most of the COVID-19 deaths in these states over our sample period. The states where we have been unable to obtain deaths by death certificate dates tend to be smaller and to have had relatively fewer COVID deaths. Typically, they did not face large peaks, which appear to be associated with increased testing delays. However, we have been unable to obtain this data from three large states – California, Illinois, and New York – and of the 20 observations (out of 4,567) with residuals from Eq. 1 whose absolute value is 50 or more, over half are from these three states.

The methods for collecting data backed by death certificates varied based on how the individual states chose to present them. Some states publish their counts based on death certificates in a downloadable format on their official COVID-19 website. Others publish them inside of longer reports in such a way that they can be hard to find, or present tables or graphs that need to be extracted by hand into spreadsheets. Because there are no official rules for how to publish this information, even the charts themselves vary in structure and presentation. Commonality across states is largely dependent on the specific software vendor they are using for their public-facing COVID-19 dashboards. Data collection procedures sometimes required hunting through source code to find full datasets within, or by hovering cursors over each bar in a bar chart individually over the collection window to make them display the precise value represented. In each case we were able to verify via labeling or official statements that the data was compiled using verified death certificate dates. It's worth noting here that, while the CDC collects deaths by death certificate date (https://www.cdc.gov/nchs/nvss/vsrr/COVID19/index.htm), they only do so at the weekly level making it unusable for the sort of modeling effort we have undertaken and, relative to the data we have obtained from individual states, suffers from even longer reporting lags.

For states where deaths by death certificate date were not available, we first sought to determine if an individual state, either on their COVID-19 reporting "dashboard" or in a downloadable file, had deaths by reported date. These datasets often contain substantial corrections to what a state originally reported on a specific day. These include reports that missed covidtracking.com's daily reporting deadline, more accurate end-of-day tallies (e.g., late reporting counties/hospitals), the correction of testing dumps that resulted in the appearance of spikes on certain days, the removal of duplicate death certificates, and the resolution of probable cases. When these differed from the COVID-19 death counts originally reported (COVIDTracking.com has a set of "snapshots" of the originally reported information) we used the updated state data. In some smaller states we believe, but have been unable to fully verify, that these corrected datasets are "close" to deaths by death certificate date.

Two of these types of corrections turn out to be particularly important. First, when a state misses a reporting deadline, this is typically recorded as there having been no COVID-19 events (new deaths positives, or tests) on that date. This causes the next day to contain the events that happened during the previous day. Second, "probable" cases have often been treated differently across states and time. State-level resolution of this issue removes an extraneous source of variation. As with the data on death certificate dates, these corrections by states of their originally reported COVID-19 statistics were obtained through a variety of sources, ranging from reading counts off interactive bar charts to downloadable CSV files.

Next, we corrected two obvious problems with the data. First, occasional, exceptionally large spikes accompanied by auxiliary information (e.g., a news/twitter release by the state's department of health) noting that this spike was due to an accumulation of deaths over an extended time period, typically from one or more congregate living facilities, e.g., nursing homes and prisons. For these, the initial correction involved proportionately increasing death counts over the relevant period, with days where this would result in negative death counts not included in the reallocation. Second, we corrected reports of zero deaths on days surrounded by death counts that were sufficiently large that a zero-death count was highly unlikely. Such days are generally also characterized by a failure to report some other COVID-19 statistics (like new positive cases) and by an abnormally high death count on the following day (or two if it is a weekend). Our approach for these was to assume no reporting followed by backlogged reporting so that the indicated correction is to average counts across the two and, in some instances, three days.

We also corrected data in situations where a state had "corrected" an earlier report, but where an entire rectified data series from the state was not available. A typical example is a state that initially reported all deaths except for those in the state's largest county, with the corrected version containing the death count for the whole state contained in a press/twitter release. A similar situation was when the data failed a logical consistency check by having the difference between the reported cumulative death counts on two consecutive days generate a negative daily death count. This typically occurs in states with small populations and few COVID-19 deaths, who, without comment, reduce their cumulative death count by one or two. Here we "rollback" that correction to the closest date that no longer produces a negative daily death count.

Similar corrections have been made to daily positive case counts and new daily test counts. The major difference is that very few states have made available positive case counts by day of test administration (rather than the day the test result is reported). This means that few states publish datasets that can readily subsume the positive case count data from The COVID Tracking project.

This is likely due to these types of information having different reporting standards. Specifically, a state eventually knows the recorded date of COVID-related death, but this information is subject to reporting delays due to waiting for confirming test results or autopsies. Because the date of death is on the death certificate, obtaining official death counts for all states is eventually feasible. However, while the lab doing the test knows the date of test administration, this information is often not shared with the state. States could require more complete reporting, but it is unclear whether the past is capturable. Total test counts are even messier due to the common practice – particularly in the earlier part of our sample period – of reporting all newly returned positive test results daily but reporting negative results inconsistently or in batches. Some negative test results (often by the state's lab) were reported along with the positives, while other negatives (often those by private labs) were reported once a week. We performed rollbacks of antibody tests that, for a while, were mixed with diagnostic tests, but these are messy because information on the period over which antibody tests were included has rarely been disclosed. We have endeavored to average and prorate testing data where the nature of this practice could be reasonably inferred.

The influence of our data correction efforts can quickly be gleaned from Table A5, which describes four simple autoregressive models with a constant term and 7th death count lag. The first uses the original "Reported" dataset (covidtracking.com) as both the source of the dependent variable, $CTPDailyDead_{it}$ and the lagged death count. The second uses our corrected version as the "Revised" for the dependent variable and uses the originally Reported for the lagged regressor. The third uses $CTPDailyDead_{it}$ as the dependent variable and the Revised for the lagged regressor. The fourth uses Revised for both. The parameter estimates for lagged deaths are similar in versions using the same lagged variable and substantively larger in the two versions using lagged revised counts. The R^2 starts at 0.69 for the Reported/Reported model, stays roughly the same (0.68) if Revised are predicted from $CTPDailyDead_{it-7}$, and increases somewhat further to 0.74 for the Reported/Revised combination. The Revised/Revised combination, though, has an R^2 of 0.91, which clearly illustrates that the large gain in explanatory power in the base Eq. (1) model in Table A1 comes mainly from our data repair and rectification effort. Note that the models in Table A5 do set the massive NJ (June 25) reported death count outlier of 1877 (Revised death count is 16) to missing, since it is so large many modeling groups have either dropped it or prorate it over earlier time periods. The R^2 of this Reported/Reported model using these observations falls to 0.42.

Temporal misalignment of $NewPositives_{it}$ has received more attention than $DailyDead_{it}$ because of the often-large gap in time between when a diagnostic test is administered and when the result is returned *(24)*. Indeed, this gap, coupled with different state testing regimes, has led most modeling groups to concentrate on predicting $DailyDead_{it}$. We have made substantial repairs to $NewPositives_{it}$ and $NewTests_{it}$ data by reference to corrected state reports, and prorated rollbacks of initially reported antibody tests. We have been much less successful in locating information on $NewPositives_{it}$ by date of test administration. However, temporal misalignment of the $NewPositives_{it-k}$ is somewhat less important than for deaths than it might first appear because there is a shorter window for positive-to-positive transmission than the positive to death transition and because test results for hospital patients, the persistent high positivity pool, are typically returned quickly. Further, even very noisy testing information can be helpful in serving as controls for variation in state-level testing behavior over time.

Construction of Temperature, Humidity and Ultraviolet Radiation Data

Weather data for our main analysis are drawn from the National Centers for Environmental Information (NCEI) Integrated Surface Database (ISD), which report hourly temperature and humidity data for most airports in the world. For each state, weather variables are taken from the airport with the highest volume of commercial traffic, where the volume information is found in the Federal Aviation Administration's 2018 Commercial Service Enplanements report. Our key variable of interest is daily maximum temperature (MaxTemp). We also look at measures of humidity and ultraviolet radiation. Hourly relative humidity is calculated as a function of hourly observed temperature and dewpoint temperature. Under the assumption of ideal gas behavior, we calculate hourly absolute humidity as well (details can be found at https://www.hatchability.com/Vaisala.pdf). We then pick the highest readings within each 24-hour period as daily MaxTemp, MaxRelativeHumidity and MaxAbsoluteHumidity. Minimum daily temperature is obtained by picking the lowest reading and the mean by averaging the hourly readings. Our measure of ultraviolet radiation is UV index, which provides a forecast of the expected risk of overexposure to UV radiation from the sun. UV index data at our representative airports was obtained from OpenWeather Ltd., which publishes daily UV index forecast calculated by the National Weather Service.

To calculate the expected date by U.S. county for entering the 5-10°C range (Figure 6), we use reanalysis data provided by PRISM Climate group (https://prism.oregonstate.edu/) which provide reliable weather data at a high spatial resolution of 4km by 4km for the contiguous U.S. We extract daily maximum temperature from 1990 to 2019 and count the average number of days it takes since Oct 1 for the daily maximum temperature to fall below 10°C.

Modelling Approach

There are two competing modelling approaches to predicting future COVID-19 deaths and positive cases. The first builds on a standard SEIR model; the other, a production function approach. The first has a strong epidemiological conceptualization and is clearly better in the early phase of a pandemic when data is scarce. The second is largely agnostic as to the underlying structure of transmission but requires dramatically more data to offset this flexibility. We follow the second, with (Eq. 1) using a simple production function approach. Conceptually, there is an infection pool with the seeds planted and various inputs (ranging from a state's health care system to temperature) that influence the output: the number of deaths observed today. We primarily use past death counts as the infection pool proxy, take into account state-level fixed effects (amalgamating effects due to constant factors such as demographic characteristics, fixed resources like health care and transportation networks, and average differences in factors including climate variables and mobility), and a simple quadratic time trend. We exponentiate the right-hand-side variables to effectively impose the restriction that under the conditions we observe, expected death counts must be non-negative.

The use of a multiplicative scaling function incorporates the logic that temperature by itself cannot generate changes in $DailyDead_{it}$. Because those dying at *t* became infected not on one day but rather over an extended period, some means of representing temperature in this setting is required. The two options, due to the strong correlation between closely adjacent $MaxTemp_{it-k}$, are a distributed lag structure that imposes structure on a set of $MaxTemp_{it-k}$, or parameterizing the scaling function as the product of individual scaling functions, each with a different $MaxTemp_{it-k}$.

We find two lags – the 7th and 14th – are sufficient and reasonably consistent with what is known about the biology of the virus and its methods of attack.

Model results are reasonably robust to small shifts in temperature lag positions, with the following two caveats. First, the 7th lag is a natural one to use; many people's lives follow a typical weekly pattern of contacts and activities, and administrative reporting procedures often have a day-of-the week pattern. Second, lags too far back are insignificant. Notably we use the 18th lag of $MaxTemp_{it}$ in the weekly model rather than its naturally shifted counterpart $LogMaxTemp_{it-21}$.

The most commonly used scaling function for our purposes is the logistic function $1/(1 + EXP(X)^{\curlyvee})$, where X is the variable of interest, and $\curlyvee$ is the single estimated parameter. This function converges to a constant as $\curlyvee$ goes to zero. Use of $MaxTemp_{it}$ rather than $LogMaxTemp_{it-k}$ as the stimulus variable provides a function with a different curvature. Statistically, it provides a similar fit, largely because the corresponding shifts in the estimate of $\curlyvee$ makes the two scaling functions reasonably similar after normalization.

We also consider another commonly used scaling function, $X/(X + \psi)$, where an estimate of $\psi > 0$ results in smaller values of X being scaled up more than large values of X and an estimate of $\psi < 0$ results in larger values of X being scaled up more than smaller values of X, and an estimate of $\psi = 0$ results in a function exhibiting no temperature responsiveness. This function can be used with either $LogMaxTemp_{it-k}$ or $MaxTemp_{it-k}$, and both will approximate a reasonable range of weakly monotonic scaling functions. It is well behaved as long as the estimate of $-\psi$ is bounded away from MIN(X), which appears not to be an issue in the situations we examine. Table A4 provides estimates for a set of competing specifications and their TRPs are displayed in Figure A8.

Our first major empirical decision was to use the three-month period of April 16-July 15. This time window allows for the seeding of the virus (to different degrees) across the i=1, …, 51 U.S. states (including DC) over a three-month period. We effectively start tracking the observable outcomes, deaths, positive cases, and tests on April 9th, because we generally use a one-week lag of the COVID-19 statistics of interest. Our time variable, t=1, …, 137 denoted in days starts with 1 on March 1st, the approximate date individual states first started reporting COVID-19 statistics.

Our second major decision involved how to implement the core epidemiological concept of a pool of infected individuals who can potentially infect other individuals. This pool is dynamic; existing positives transition to being no longer infectious, while newly infected individuals enter the pool. The totality of the currently infected individuals is unobservable without universal administration at each point in time of a 100% accurate diagnostic test. The question, thus, is whether to use a lagged variant of the test diagnosed positives, $NewPositives_{it}$, which logically are part of the infection pool but not necessarily representative of it due to differential testing, or a lagged variant of $DailyDead_{it}$.

The lagged $DailyDead_{it}$ measure is one step removed but was previously assumed to always be observed *(25,26)*. This assumption is demonstrably false. In the early run of the pandemic many deaths failed to be classified as COVID-19-related, in part because some instances were thought to be influenza-related, while COVID-19's role in inducing cardiac and kidney failure was not widely recognized. We avoid many of these problems by only using $DailyDead_{it}$ data generated after the pandemic was well established.

Other problems with using lagged $DailyDead_{it}$ (or $NewPositives_{it}$) as the infection pool indicator (such as a state having a proportionately larger elderly or disadvantaged population) are readily addressed using the standard statistical approach of including time-invariant state-level fixed effects.

One way the use of a lagged version $DailyDead_{it}$ vs. $NewPositives_{it}$ will vary is with respect to timing. Current positives are temporally closer to future positives or deaths than current deaths and can potentially pick up the virus spreading among healthy young adults. The shorter link between a lagged $NewPositives_{it}$ is enhanced by the short period over which a current positive can influence future COVID outcomes, which makes TRP estimation less sensitive to the choice of temperature lags.

Subject to the same measurement error, using $NewPositives_{it-7}$ should be preferred to $DailyDead_{it-7}$ as the infection pool indicator. These results are provided in Table A6 (Model 16). The main lesson is that the model using $LogNewPositives_{it-7}$ is a good predictor of $DailyDead_{it}$ ($R^2 = 0.94$), but not as good as $LogDailyDead_{it-7}$. This suggests that either the positives have more measurement error than our corrected version of death counts or that the $DailyDead_{it-7}$ is a better reflection of the current risk-adjusted infection pool than $NewPositives_{it-7}$. The other result worth noting is that with the infection pool indicator temporally advanced, the coefficient on $LogMaxTemp_{it-14}$, as expected, is no longer significant.

The parameter estimates for the base model (Table A1) can be used to provide an estimate of the minimum infection pool each state faces by setting $DailyDead_{it-7} = 0$ (from a statistical perspective), obtaining expected $DailyDead_{it}$, and dividing it by the CDC's point estimate of the infection fatality rate (0.0065) *(27)*. Setting the value of $Days_t$ equal to the end of the sample period, across states, the sum of these minimum infection pools is 9853 cases. Figure A3(A) provides a visual display of this information for the continental U.S. states.

Interpretation of State-level Fixed Effects and Time-Related Effects

We calculate a variant of the state-level fixed effects from our main regression model (Table A1) by setting the time trend equal to the last day of our sample period, the lagged number of deaths equal to zero, and calculating the expected number of deaths for each state. Small, isolated states like Hawaii generate estimates close to zero while the most populous states tend to generate estimates above 2. These estimates suggest the minimum infection pool in each state varies by a factor of approximately 20 (Figure A3(A)). A regression (Table A3) of the minimum expected death count on a small set of state-level demographics taken from the U.S. Census Bureau (LogPopulation, %Black, %Hispanic, and %Age80+) explains 79% of the variation in these counts.

We do not want our TRP estimates to be confounded by other factors changing over time (ranging from state and locally mandated shelter-in-place orders, reopening plans, endogenous social distancing, propensity to wear face masks and changing fatality rates). Since we are agnostic as to the mechanism, the straightforward specification is a polynomial time trend, where we find a quadratic term justified. Higher order terms add little insight or predictive power. The quadratic trend for predicting $DailyDead_{it}$ falls sharply from mid-April to the end of May, after which it very slowly starts to turn up.

A model which adds (a) the number of days since a state issued a mandatory shelter-in-place order and (b) the number of days since a state started to formally reopen its economy can be found in

Table A6 (Model 8). The coefficients on these two variables are small and insignificant. The two $LogMaxTemp_{it-k}$ parameters fell on average by less than 1%.

This might seem puzzling until it is recognized that the two sets of time-related variables are highly correlated. Dropping the quadratic trend (Model 9 in Table A6) provides a different picture because, while still statistically significant at conventional levels, it was substantially diminished. The earlier a state shelter in-place order was issued, the lower the predicted death count ($p = 0.028$), and the earlier a state started to reopen the higher the predicted death count ($p < 0.001$). We are reluctant to provide any substantive interpretation to this result. Papers that have tried to determine the role of state actions and the behavior they are intended to influence show the need to (a) extensively model both state and local orders, and (b) incorporate spatially disaggregated mobility data in order to identify the effects of these government mandates from endogenous social distancing by the public that often occurs before these actions *(28,29,30)*. The two temperature coefficients in this model fall on average by less than 20% and remain highly significant.

Alternative Specifications for Base Death Count Model

Table A4 compares our base model to alternative specifications. These alternative specifications were chosen to look at the sensitivity of the implied TRP because they all have reasonably similar fits relative to our base model. This allows us to observe how robust the TRP is to a substantial shift in various modelling decisions that we made. The first specification replaces the $LogMaxTemp_{it-k}$ with their linear counterparts. On the surface, this seems like a decision about which of two different scales fits better, but because the models have estimated parameters in the scale function, it may be possible for the two different specifications to provide reasonably similar TRPs. The second uses a popular ratio scaling function $LogMaxTemp_{it-k}/(LogMaxTemp_{it-k} + \alpha)$, where α is an estimated parameter. The third replaces $LogMaxTemp_{it-k}$ with $MaxTemp_{it-k}$ in this ratio scaling function. A potential issue with Eq. 1, is the possibility that $LogMaxTemp_{it-14}$ directly influences our main infection pool indicator $LogDailyDead_{it-7}$. Our next specification replaces our infection pool indicator with an alternative, $LogDailyDead_{it-14}$, so both temperature variables are now clearly exogenous from the temporal perspective of the infection pool indicator.

The last is a weekly variant (Eq. 2) of the base model, where the dependent variable is the sum of the daily death count of the next seven days with corresponding pushbacks of the lagged variables. This model averages out much of the daily variation and many types of administrative reporting practices. In forecasting the pandemic's progression, it has become common to use data aggregated to a weekly level in an effort to average out many of the administratively-induced reporting issues that our extensive reconstruction and repair of the daily death count data sought to alleviate. It is possible to estimate a variant of Eq. (1) that uses death count data aggregated into seven-day periods, $WeeklyDead_{it} = \Sigma_t\, DailyDead_{it}$, where the summation is over t=1 to t=7. This makes $WeeklyDead_{it-7}$ the sum of the 7th through 13th lags of $DailyDead_{it}$. Importantly, this aggregation does not reduce the number of observations because on each day, the weekly aggregation at t=1 adds a new observation $DailyDead_{i1}$ and drops $DailyDead_{i8}$. Lags of the $WeeklyDead_{it}$ variable can then be used in the standard way. One implication of this specification is that the temperature variables also need to shift backwards. For conceptual consistency, we use $LogMaxTemp_{it-14}$ in place of $LogMaxTemp_{it-7}$. Empirically, the model fits best with the second temperature lag being $LogMaxTemp_{t-18}$. The model fit is reasonably similar using the 13th lag and 19th lags, but beyond the 19th lag, the temperature variable becomes insignificant, suggesting temperature information farther back in time than this is not useful. The model we report is thus:

$$WeeklyDead_{it} = EXP(\Sigma_i\ StateIndicator_i + \alpha_1 LogDays_t + \alpha_2 LogDays_t^2 + \beta LogWeeklyDead_{it-7})$$
$$*(1/(1 + EXP(LogMaxTemp_{t-14})^{\acute{}\Upsilon 1}))*(1/(1 + EXP(LogMaxTemp_{t-18})^{\acute{}\Upsilon 2})) + \varepsilon_{it}. \quad (2)$$

The overall impression from Table A4 is the general stability of most of the common parameters for time and the infection pool. Some of the specifications offer insights into the latter variable. It is little influenced by whether the logistic or ratio scaling function was used, nor whether $LogMaxTemp_{it}$ or $MaxTemp_{it}$ was the stimulus variable. Using $LogDailyDead_{it-14}$ in place of $LogDailyDead_{it-7}$ results in an estimated TRP being similar to the base model (Figure A6), although it does rise more sharply between 10°C and 5°C suggesting, while there may be a endogeneity effect, it is not large and that our base TRP is conservative. In this model (Table A6, Model 7), the coefficient on the infection pool indicator shifts from the .86 of the base model to .80; in the weekly version model it jumps to .92, The R^2 for the weekly model increases to 0.99 (from the base model's 0.97) and falls to 0.94 in the model using $LogDailyDead_{it-14,}$ which is less informative than $LogDailyDead_{it-7}$ in term of the infection pool influencing current death counts .

Constructing Temperature Response Profiles (TRPs)

To compare the TRP's implied by the models in Table A4, we plot the functions using two independent random uniform variables RTemp and RTemp2, defined over the range 5°C and 40°C. The logistic scaling function with two temperature variables, $LogMaxTemp_{it-7}$ and $LogMaxTemp_{it-14}$, and corresponding Eq. 1 estimated parameters ΄Υ1 and ΄Υ2 (Table A4), results in the following scaling function in the base model:

$$(1 /(1 + \exp(LogRTemp^{\acute{}\Upsilon 1})))*(1 /(1 + \exp(LogRTemp2^{\acute{}\Upsilon 2}))). \quad (3)$$

There is a fundamental indeterminacy in such a scaling function, in that multiplying the production function part of Eq. 1 by a constant will result in an offsetting change in the scaling function which maintains the same expected value for the dependent variable. Note that each of the two multiplicative components of Eq. 3 converges to .5 irrespective of temperature values as ΄Υ1 and ΄Υ2 become increasingly negative. Often logistic functions are normalized to lie between 0 and 1 by changing the "1" in the numerator to "2", but this is not needed with our normalization to 31°C, which solves the indeterminacy from the perspective of comparing curves. This is done by calculating the value of the estimated scale function at 31°C:

$$(1 / (1 + \exp(\log(31)^{\acute{}\Upsilon 1})))*(1 /(1 + \exp(\log(31)^{\acute{}\Upsilon 2}))). \quad (4)$$

Dividing Eq. 3 by Eq. 4 produces a function which equals 1 at 31°C. Multiplying this quantity by 100 produces a function which has a natural percentage interpretation and equals 100 at 31°C. Note that for forecasting purposes, the original scaling function parameters need to be used.

The ratio scaling function with estimated parameters α_1 and α_2 using RTemp and RTemp2 is:

$$(LogRTemp/(LogRTemp + \alpha_1)) *(LogRTemp2/(LogRTemp2 + \alpha_2)). \quad (5)$$

As α_1 and α_2 converge to zero, both multiplicative components of SI.1c converge to 1 irrespective of temperature values. The value of this function at 31°C can be calculated in a manner similar to that described for the logistic. Dividing Eq. 5 with the value of that function at 31°C and multiplying by 100 produces the desired TRP.

Figure A8 graphs the daily death TRPs from the model specifications in Table A4. The alternative specifications produce TRPs remarkably similar to that of our base model and tend to bracket it.

The one systematic difference is that TRPs based on the ratio scaling functions tend to be flatter over 10°C to 20°C but rise more sharply in the 5°C to 10°C range.

Further $DailyDead_{it}$ Specifications Involving Weather, Positives and Cumulative Dead

The other weather variables which have received considerable attention are absolute humidity, relative humidity, and ultraviolet (UV) radiation. Details of construction are provided below in Data Preparation Section. The limitation with all these variables is that they are correlated with $MaxTemp_{it}$ (i.e., absolute humidity: 0.58, relative humidity: -0.21, UV: 0.79). Maximum absolute humidity has a reasonable size effect ($p < 0.001$) in the model where it replaces the corresponding $MaxTemp_{it}$ variables. However, the $LogAbsoluteHumidity_{it-k}$ parameter estimates are close to zero and are no longer significant when the two parallel logistic functions comprising the temperature scaling function are added (Model 10 in Table A6). Relative humidity has a marginally significant relationship with $DailyDead_{it}$ when $MaxTemp_{it}$ is not in the model and its effect is close to zero in a model with $MaxTemp_{it}$ (Model 11 in Table A6).

The situation with UV_{it} for which (15) found support is more complex (Table A4 &Table A6, Models 12 and 13). The $MaxTemp_{it}$ lags are marginally better predictors in a head-to-head comparison. These two variables are strongly correlated. Adding UV_{it} marginally decreases prediction errors, but the signs of high multicollinearity are obvious; the first $MaxTemp_{it}$ lag is still highly significant while the second is insignificant and one of the UV_{it} lags is only marginally significant (Table A4). It is effectively impossible to disentangle the influence of $LogMaxTemp_{it}$ and UV_{it}. Their relationship is displayed in Figure A5, which plots $LogMaxTemp_{it}$ and $LogUV_{it}$ for two states over our sample period: Georgia (Atlanta) and New York (New York City). We cast our results in terms of $MaxTemp_{it}$ rather than UV_{it} because it is more widely reported and understood, without making any claim our work supports a joint versus singular causal mechanism.

The specification in Eq. (1) is cast in terms of $DailyDead_{it}$. If $MaxTemp_{it-k}$ influences COVID transmission via the link between positive cases, then we should be able to replace $DailyDead_{it-7}$ with $NewPositives_{it-7}$. Estimates for this model (Table A4) show $LogNewPositives_{it-7}$ being significant at $p < 0.001$ and the R^2 measure falling a bit. The coefficient on $MaxTemp_{it-14}$ is insignificant, which would be expected if $NewPositives_{it-7}$ incorporates that information, while the coefficient on $LogMaxTemp_{it-7}$ is larger than in the base specification.

A different aspect of the COVID-19 death statistics that has not been incorporated into the model is lagged cumulative death count, $TotalDead_{it-k.}$ If $DailyDead_{it-k}$ can be seen as a proxy for the infection pool influencing $DailyDead_{it}$, then $TotalDead_{it-k}$ (normalized by population) is proxy for the fraction of the population that no longer at risk in the sense of being either removed by death or recovered. Adding $LogPCTotalDead_{it-7}$ effectively makes the $StateBase_{it}$ dynamic in a potentially different way than the quadratic time trend by letting each state evolve according to its own pattern of deaths. Table A6 (Models 14 and 15) displays the results of this model with $LogPCTotalDead_{it-7}$ enter as (a) a second order polynomial and (b) a fourth order polynomial.

Three results are worth noting. First, the increase in explanatory power is small with the most noticeable changes being as expected in the $StateIndicator_i$ and a substantial reduction in importance of the overall quadratic time trend. Second, the $LogMaxTemp_{it-k}$ parameter estimates are similar to that of Eq. (1) suggesting that our TRP is robust to a substantial dynamic reparameterization of the model. Third, in the quadratic specification, $DailyDead_{it}$ is declining with as $LogPCTotalDead_{it-7}$ at a declining rate. In the fourth order specification, all the $LogPCTotalDead_{it-7}$ terms are insignificant (although jointly significant). Figure A6 displays,

starting at .05, the two response functions for $LogPCTotalDead_{it-7}$. Like the quadratic time trend, they suggest a sharp drop in how $DailyDead_{it}$ is influence by $DailyDead_{it-7}$ as $LogPCTotalDead_{it-7}$ increases from low levels with the fourth order polynomial being flatter at high levels of $LogPCTotalDead_{it-7}$ than the quadratic. The influence of this factor is reasonably small by the time a state hits 10 deaths per 100,000, a condition that characterizes 80% of the states at the end of our sample period. Earlier, we noted one interpretation of the quadratic time trend was that medical care (and hence death rates) had improved sharply at first and then at a declining rate. This specification has a similar interpretation but suggests that some of that learning is state specific and related to its prior COVID-19 caseload. There is no indication that this rate of decline is accelerating even in the hard-hit Northeastern states where deaths per 100,000 can be as high as 175 (NJ), looking at the fourth order polynomial which should allow this feature to emerge if the data supports it. This suggests the magnitude of the fraction of the population previously infection is still too small to be a substantial factor in slowing transmission of the virus.

Univariate $DailyDead_{it}$ and $MaxTemp_{it-7}$ Relationship

If we have succeeded in isolating the TRP through use of the set of $StateIndicator_i$ and a quadratic time trend, the simple regression of $DailyDead_{it}$ on lagged $MaxTemp_{it-7}$ without the state fixed effects and quadratic time trend should reveal a substantially different curve than our estimated TRP displayed in Figure 4. Figure A7 displays this relationship using a robust LOWESS smoother (bandwidth 0.2) on $MaxTemp_{it-7}$. This curve is dramatically more sensitive to temperature between 10°C and 30°C. Below 10°C it drops, which was expected since states with temperatures near 5°C tend to be more isolated and smaller population-wise. The curve bends up near 35°C and beyond where most of the observations come from a few states with (relatively) high June and July death counts.

Pinning down the TRP further will require: (a) obtaining more data over a longer time horizon with more temperature variation and, in particular, the important -5°C to 5°C range, where there has been little U.S. experience since the virus became widely dispersed, (b) obtaining death certificate data information from the few remaining large states (California, Illinois and New York) where it is not yet available, since states with death certificate date reporting have prediction errors that are substantially smaller ($p < 0.001$) than those that don't (Table A6, Model 2), or (c) having high quality temporally aligned COVID-19 statistics at the county level, which would provide a better temperature match and dramatically increase sample size.

Death Count TRPs based on DailyDead vs. COVID Tracking Project Originally Reported Counts

What does a TRP based on The COVID Tracking Project's (CTP) originally reported death counts look like compared to our base (Eq. 1) Model 1 which uses $DailyDead_{it}$? To examine this issue, we estimate Model 26 (Table A6), a direct analogue of Model 1, that substitutes $CTPDailyDead_{it}$ and $CTPDailyDead_{it-7}$ for their $DailyDead_{it}$ counterparts. Consistent with Model 18 (Table A6) and other models employing $CTPDailyDead_{it}$, we exclude the two observations that contain the large New Jersey outlier as either the dependent variable or regressor and further excluded twenty observations where $LogCTPDailyDead_{it-7}$ is undefined because $CTPDailyDead_{it-7}$ is negative.

There are some clear differences between Model 1 and Model 26. First, in Model 26 there is a large drop in the R^2 from 0.97 to 0.81 and the RMSE measure more than doubles. Second, the elasticity parameter on lagged $LogCTPDailyDead_{it}$ is just over 60% as large as it is in the $DailyDead_{it}$ version. This is the expected result from introducing substantial measurement error, but one that also has large implications for drawing inferences about the size of the infection pool

or in undertaking any dynamic forecasting exercise. Third, the quadratic time trend, while still sizeable, is substantially diminished in both magnitude and statistical significance. Fourth, there are differences between the TRPs implied by their temperature response parameters in Eq. (1).

The TRPs for Model 1 and Model 26 are plotted in Figure A9. The TRPs for the $CTPDailyDead_{it}$ variant effectively lies above its $DailyDead_{it}$ counterpart. At 5°C, it predicts almost 80% more deaths than our base Model 1. This result may seem counterintuitive to the usual belief that measurement error induces the parameter estimate to be attenuated toward zero. That, intuition, generally correct, helps explain the fall in coefficient when $CTPDailyDead_{it-7}$ rather than $DailyDead_{it-7}$ is used as the infection pool indicator. However, it does not say anything about the implication of introducing measurement error into another covariate in the model. It is easy to show that as the scale of the measurement error in the lagged death count increases, the magnitude of the temperature responsiveness parameters adjusts to incorporate covariance with $DailyDead_{it-k}$. All else held constant, this would increase the magnitude of the estimated temperature effect under classical measurement error, since the parameters on infection pool indicator and temperature variables should have the same sign.

The situation here is more complicated because measurement error from using $CTPDailyDead_{it}$ also substantially reduces the ability to pin down the quadratic time trend. Thus, neither the sign nor magnitude of the difference between the temperature response parameters across comparable specifications is therefore known a priori. Our parameter estimates (Table A6) suggest an upward bias is likely in temperature effect estimates obtained from models similar to ours that (a) use reported death counts and (b) have specifications where the infection pool and temperature response variables are expected to share the same sign. Note though that in a simple OLS regression model, the infection pool and temperature variables should have opposite signs, resulting in an estimate of the temperature parameter likely biased in the direction of finding no effect.

Structure of Table A6

The parameter estimates and standard summary statistics for models discussed is this paper are provided in Table A6. It contains three columns for each model. The first column contains the variables included in the model, the second the parameter estimates, and the third the standard errors. After the parameter estimates, the model's R^2, root mean square error (RMSE), and the number of observations on which the model was fit are provided.

The order in which the models appear are:

1. The base model represented by Eq. 1 using $LogDays_t$, $LogDays_t^2$, and $LogDailyDead_{it-7}$ as the predictors along with a set of state-level indicator variables and using $LogMaxTemp_{it-7}$ and $LogMaxTemp_{it-14}$ in the temperature scaling function.

2. A model which regresses the squared residuals from (1) on the log of state population and an indicator variable, GOOD_DATE for $DailyDead_{it}$ representing death counts by death certificate date.

3. Base model using linear versions of the two temperature variables.

4. Base model using alternative ratio scaling function Temp/(Temp + α), where Temp is temperature variable and α is the estimated parameter.

5. Base model using the alternative ratio scaling function and linear versions of the $MaxTemp_{it-k}$.

6. Base model with $LogDailyDead_{it-14}$ substituted for $LogDailyDead_{it-7}$.

7. A weekly version of the base model (see Eq. 2) substituting $LogDailyDead_{it-14}$ for $LogDailyDead_{it-7}$ and $LogDailyDead_{it-18}$ for $LogDailyDead_{it-14}$.

8. A version of the base model that adds two state-level government policy variables, the log of the number of days since a shelter-in-place order was first issued ($LogDaysShelterInPlace_{it}$) and the log of the number of days since a state began to formally reopen its economy ($LogDaysReopen_{it}$).

9. A version of (8) that drops the quadratic time trend of the base model.

10. The base model adding parallel scaling functions using the $LogMaxAbsoluteHumidity_{it-7}$ and $LogMaxAbsoluteHumidity_{it-14}$.

11. The base model adding parallel scaling functions $LogMaxRelativeHumidity_{it-7}$ and $LogMaxRelativeHumidity_{it-7.}$

12. Base model adding additional parallel scaling functions for $LogUV_{it-7}$ and $LogUV_{it-14}$.

13. Base model substituting $LogUV_{it-k}$ for $LogMaxTemp_{it-k}$.

14. Base modeling adding a quadratic in terms of $LogTotalDead_{it-7}$.

15. Base modeling adding a 4th order polynomial $LogTotalDead_{it-7}$.

16. Base model substituting $LogNewPositives_{it-7}$ and testing variables for $LogDailyDead_{it-7}$.

17. The model used in the paper to predict $NewPositives_{it}$.

18. The AR(7) regression of the originally reported death counts from The COVID Tracking Project ($CPTDailyDead_{it}$) on the 7^{th} lag of itself ($CPTDailyDead_{it-7}$) for Table A5.

19. The same as (18) but with $DailyDead_{it}$ regressed on the 7^{th} lag of the $CTPDailyDead_{it}$.

20. The same as (18) but $CTPDailyDead_{it}$ regressed on the 7^{th} lag of $DailyDead_{it}$.

21. The same as (18) but $DailyDead_{it}$ regressed on its 7^{th} lag.

22. The $StateBase_{it}$ calculation for each state.

23. The model reported in Table A3 which predicts the state-level fixed-effect estimates obtained in (1) as a function of a small set of demographic variables.

24. State-level estimates of the minimum infection pool.

25. State-level change in expected $DailyDead_{it}$ when $DailyDead_{it-7}$ shifts from 0 to 1 on July 15, assuming 31°C.

26. Base model (1) using the uncorrected death count data.

Data and Code Availability

The data used in this study are archived at https://github.com/xxx in the form of a Stata ".dta" file. An Excel version of this file was created using StatTransfer. The Stata "do" file creating the data set contains a line-by-line set of the changes made to the original CovidTracking.com data set, and the providence of those changes. Three additional Stata "do" files are available in this archive. The

first contains the code (Stata 16.1) for the regression models reported in this paper. The second provides an example of how to estimate the static and dynamic temperature response profiles for an individual state using Georgia as an example. The third contains Stata code for creating the basic versions (fine labeling was done using Stata's graph editor) of the figures in this paper. We also provide a further Stata dataset and corresponding Excel files at the state level (using our representative airport) with maximum daily temperature readings from the last thirty years.

Appendix Figures

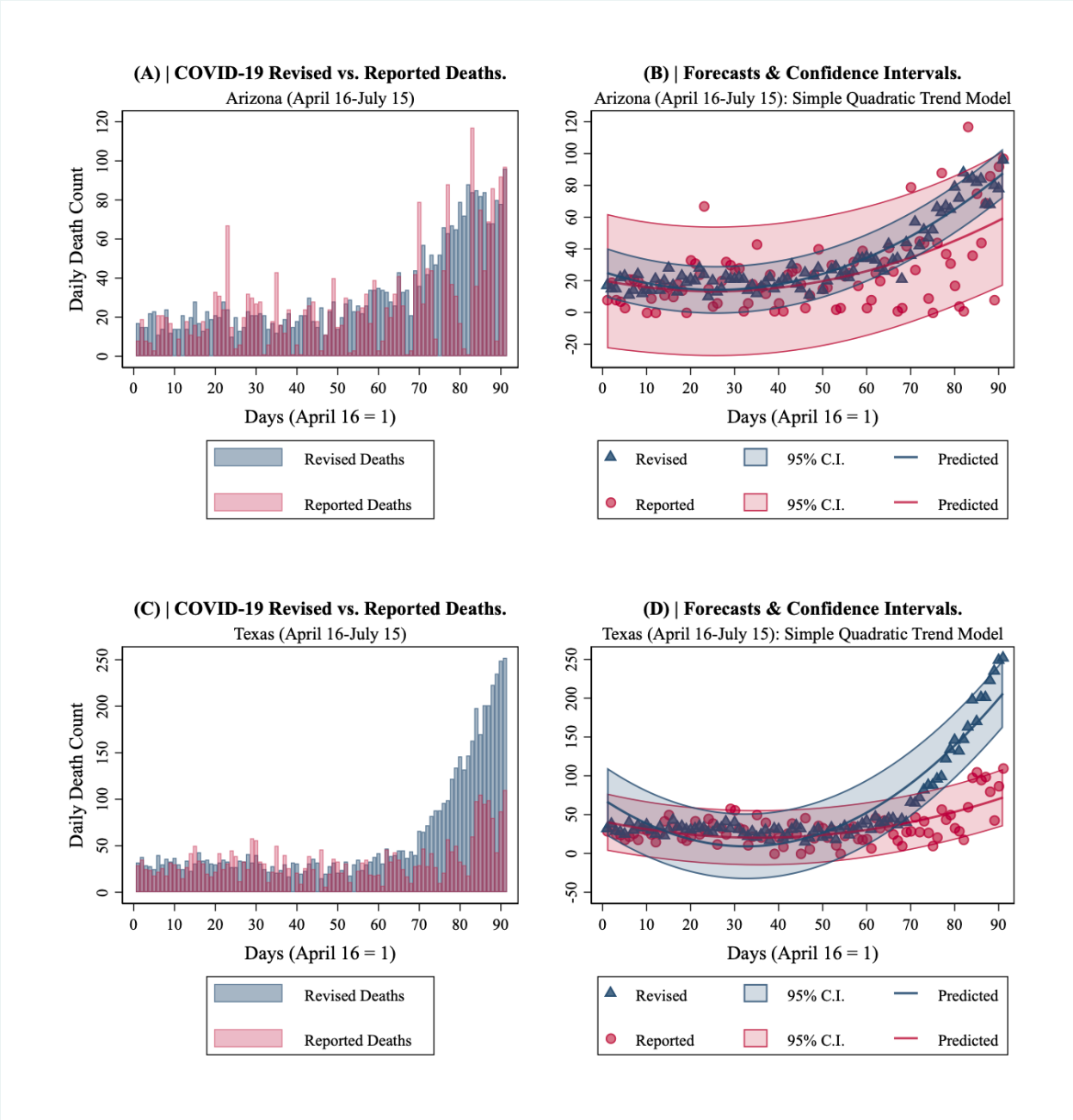

Figure A1. COVID-19 deaths in Arizona and Texas. April 16-July 15. **(A)** Arizona Revised vs. Reported. **(B)** Arizona quadratic time trend forecasts and confidence intervals. **(C)** Texas Revised vs. Reported. and **(D)** Texas quadratic time trend forecasts and confidence intervals.

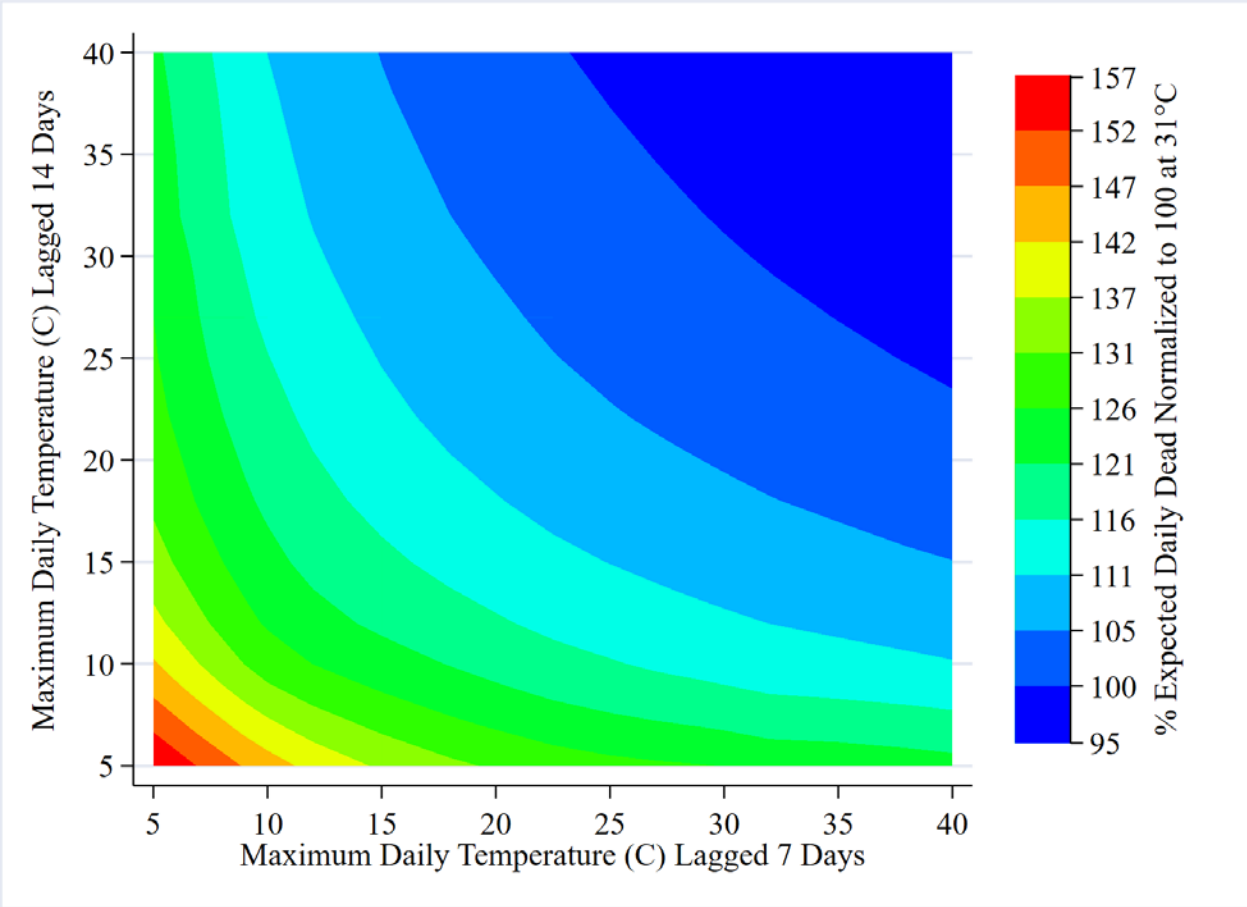

Figure A2. DailyDead TRP contour plot representation.

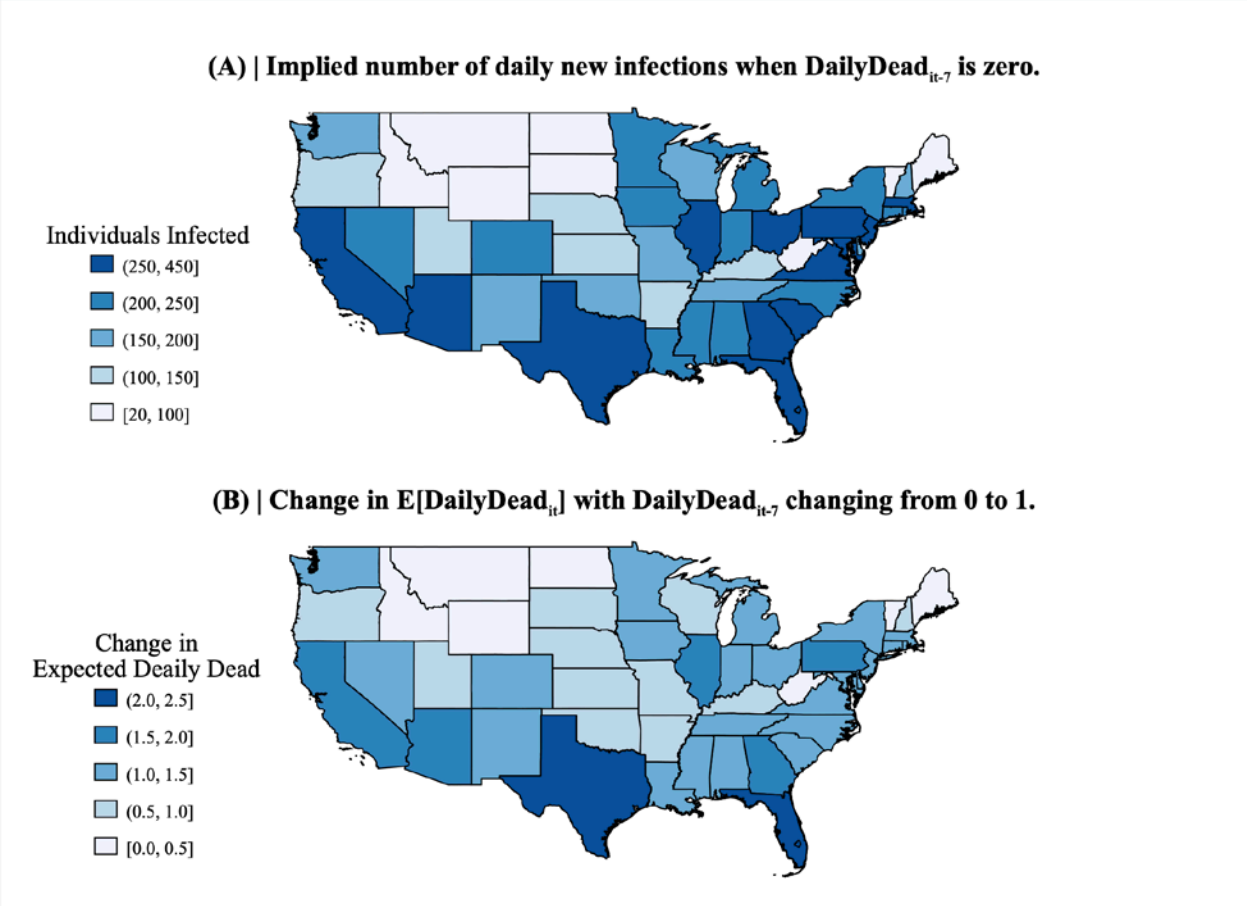

Figure A3. Visual representation of information contained in the parameter estimates for base model (Eq. 1). (A) displays the infection pool for each state in the continental U.S. implied if observed DailyDead$_{it-7}$ is set to zero on July 15 and the two lagged MaxTemp$_{it-k}$ are set to 31°C. **(B)** shows, under the same conditions, how the expected DailyDead$_{it}$ changes if DailyDead$_{it-7}$ moves from 0 to 1.

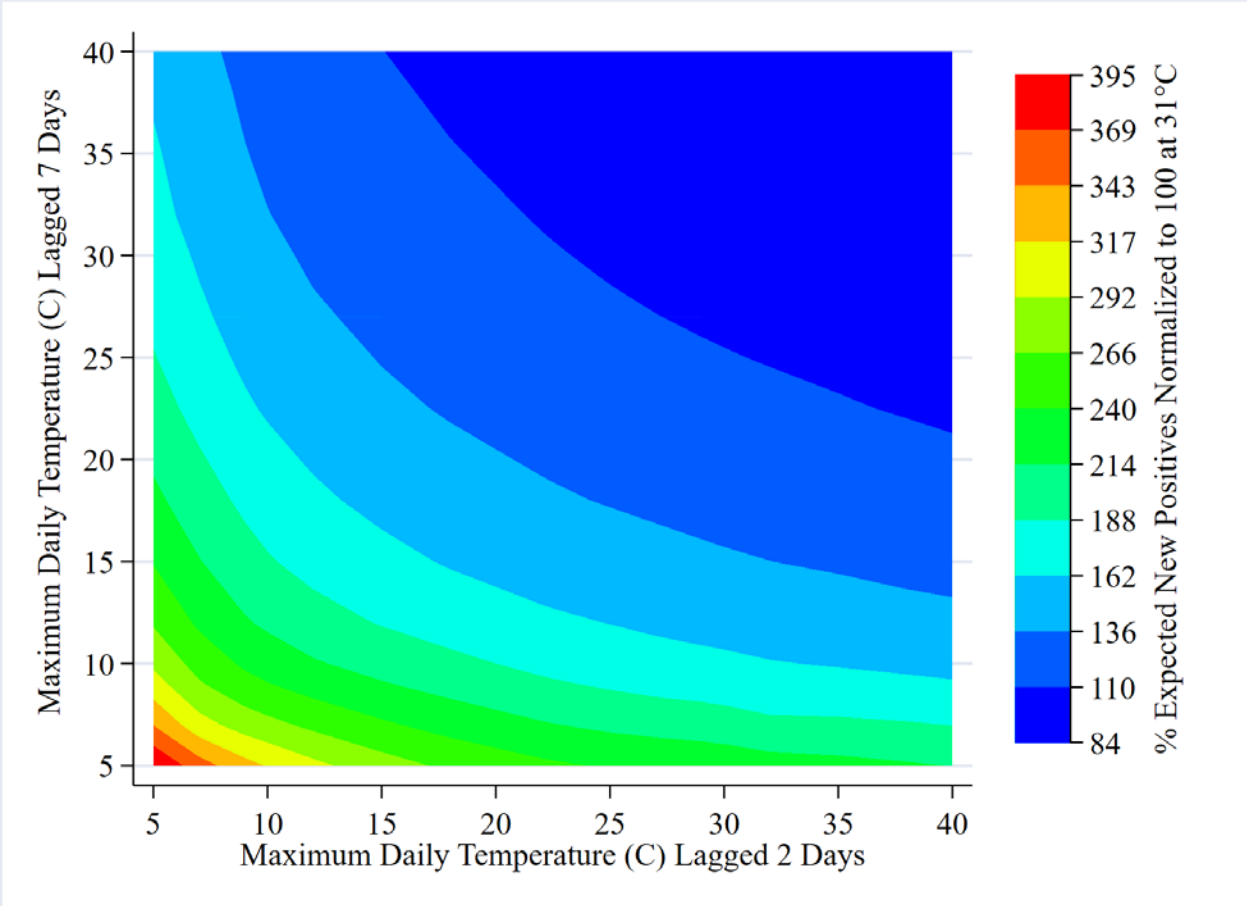

Figure A4. NewPositives TRP contour plot representation.

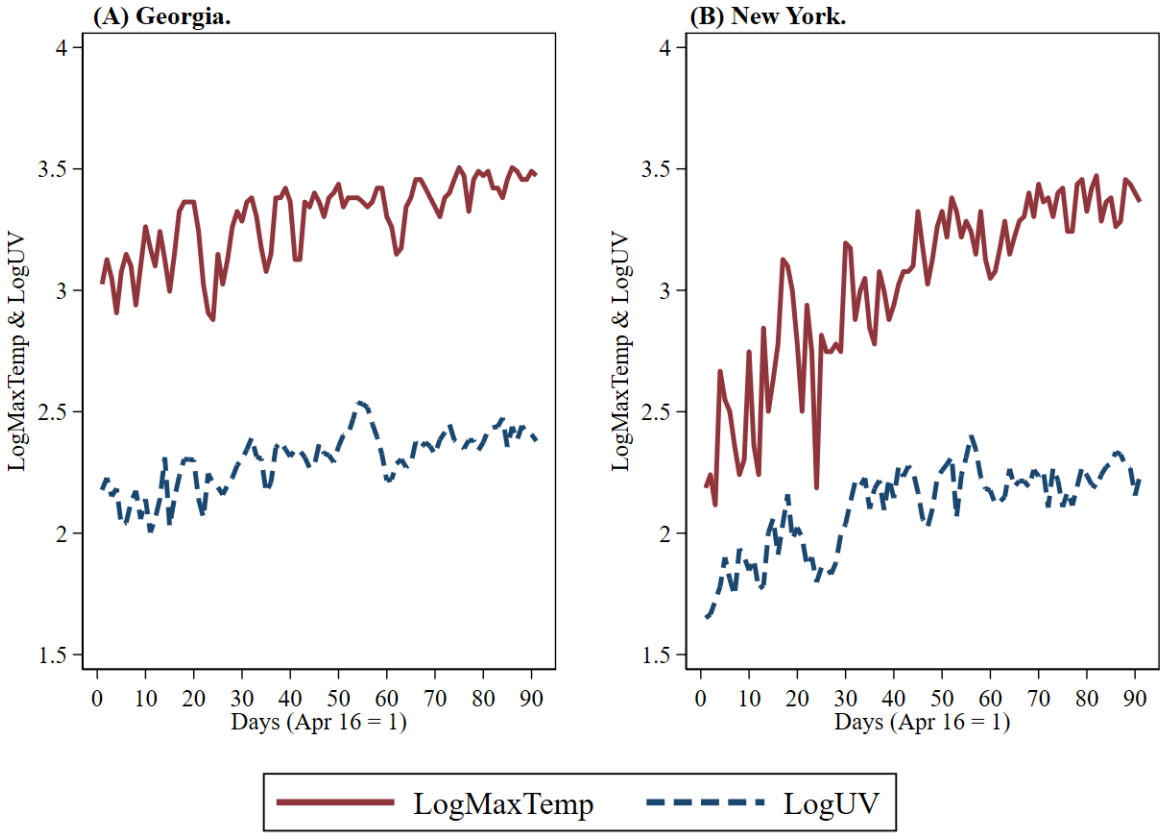

Figure A5. LogMaxTemp vs. LogUV. (A) displays Georgia. **(B)** displays New York.

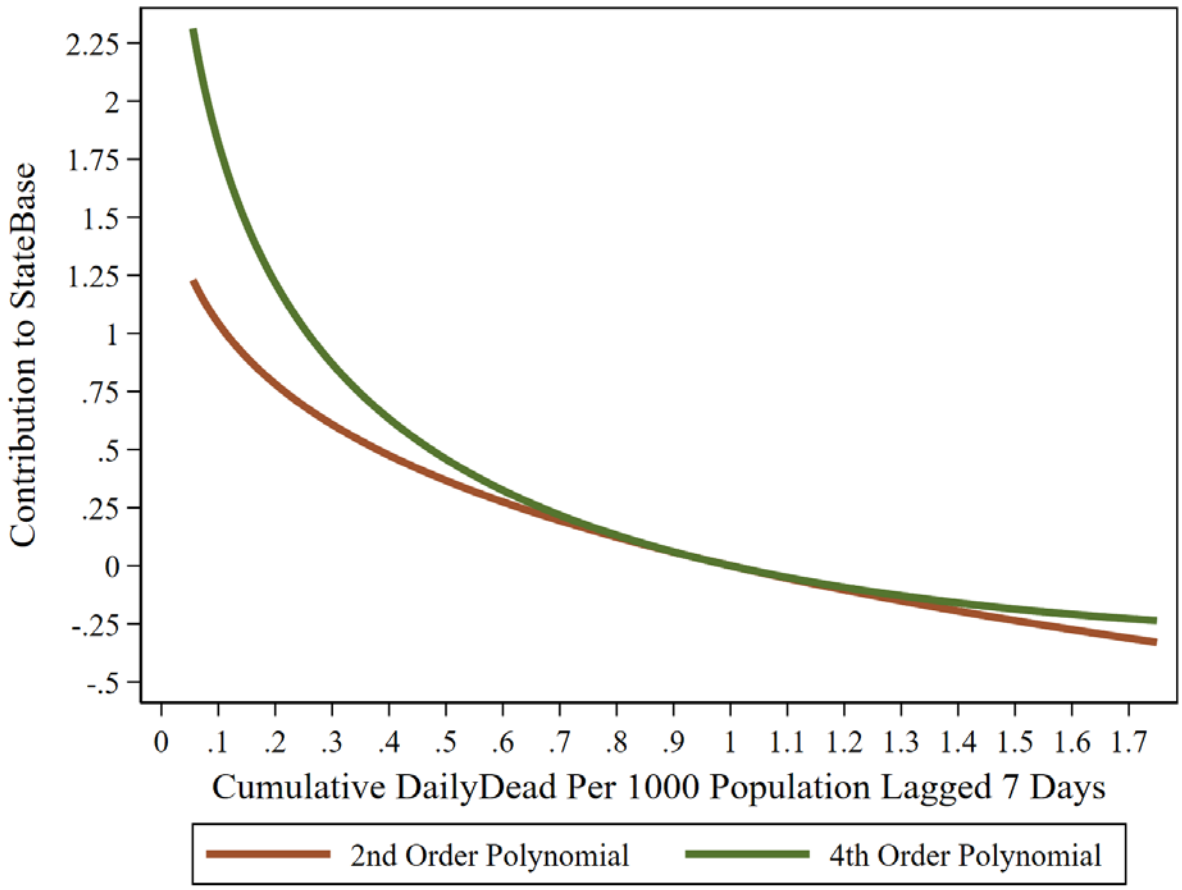

Figure A6. DailyDead$_{it}$ responsiveness to lagged per capita total dead.

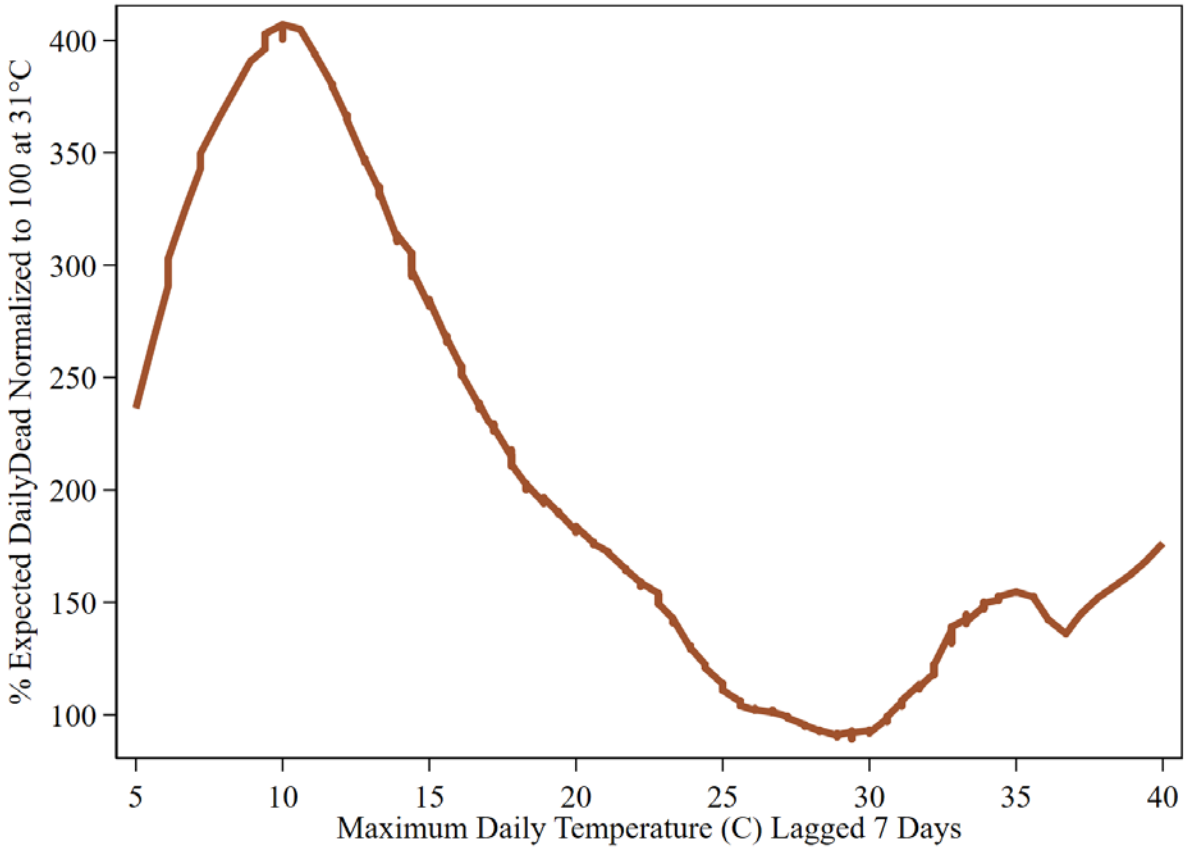

Figure A7. Bivariate relationship DailyDead & MaxTemp. U.S. states: April 16-July 15. Lowess smoother: .2 bandwidth.

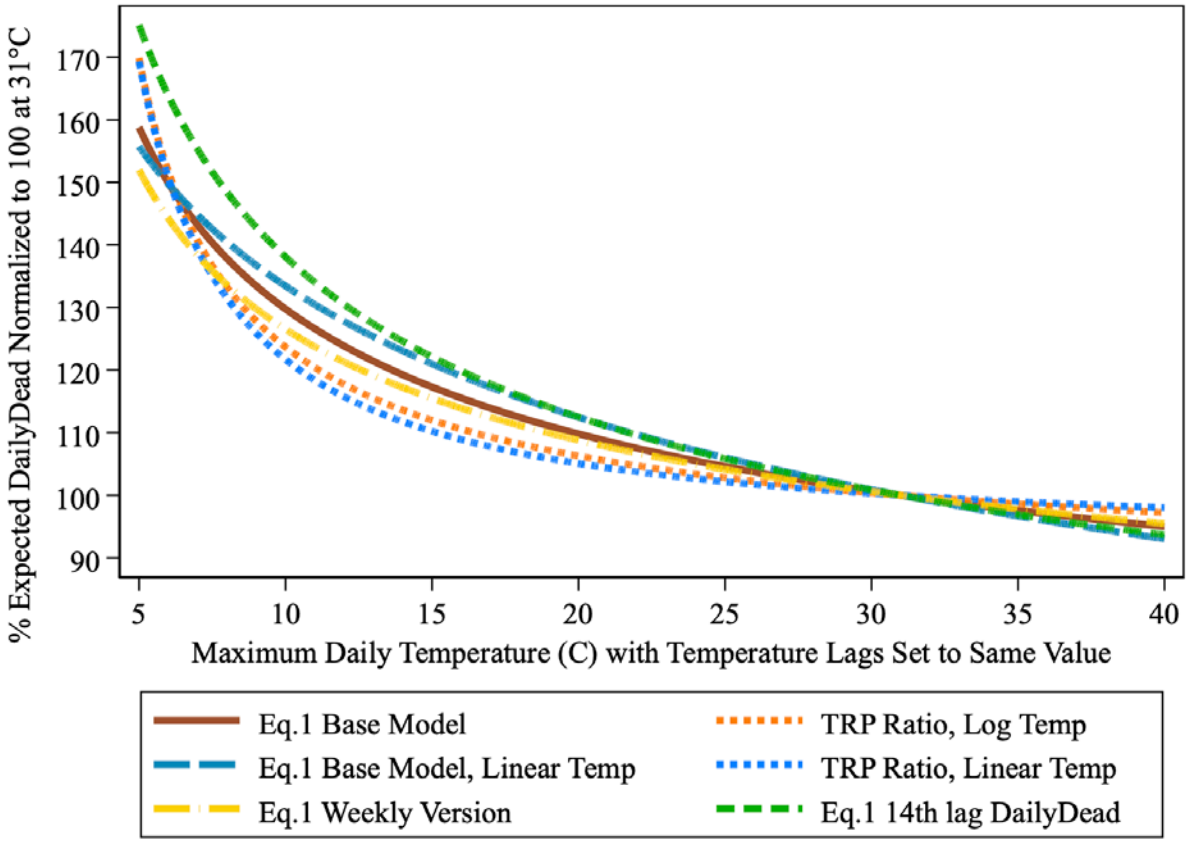

Figure A8. Alternative DailyDead TRPs. U.S. states: April 16-July 15.

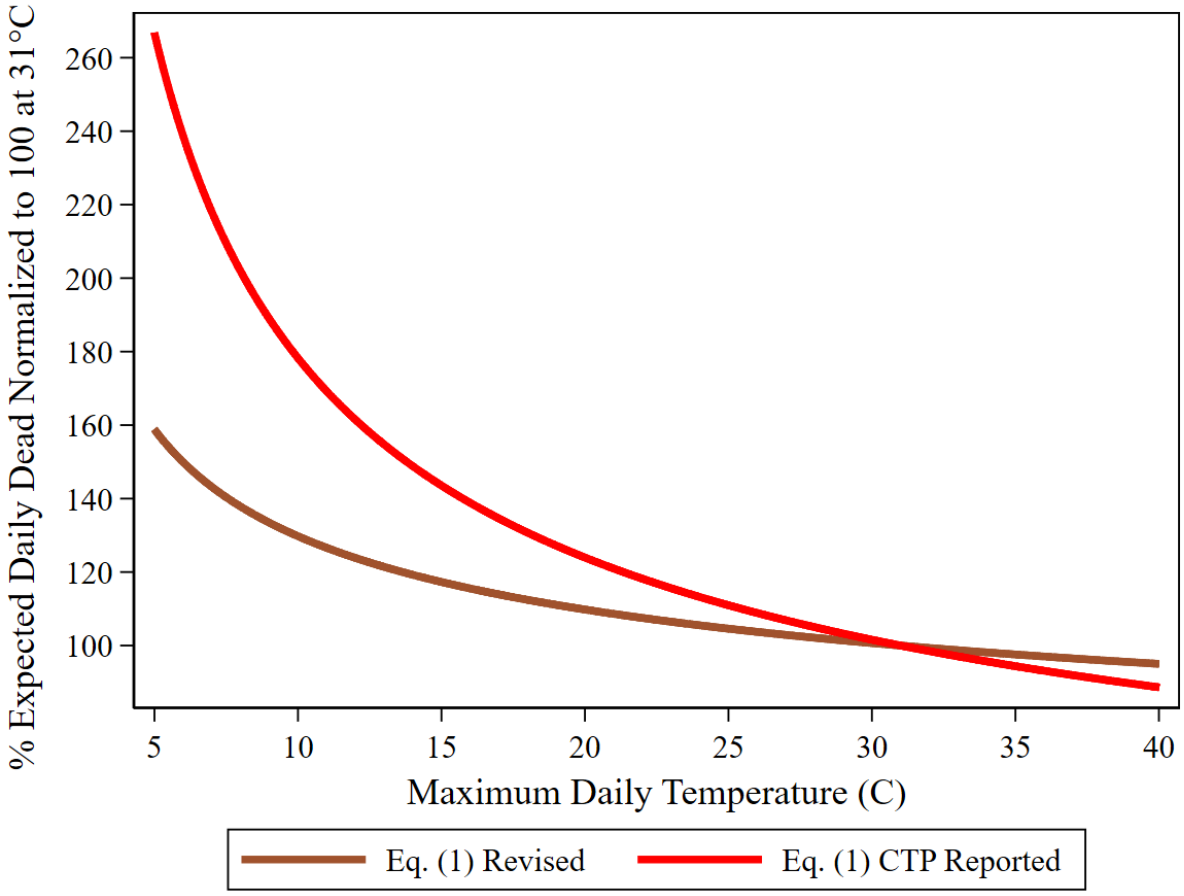

Figure A9. Death count TRPs based on DailyDead vs. CTP originally reported. U.S. states: April 16-July 15.

Table A1. Eq. (1) base model predicting $DailyDead_{it}$.

Variable	Coefficient	Robust S.E.	t-statistic	p-value
Alaska	24.2468	3.2668	7.42	0.000
Alabama	26.2830	3.2504	8.09	0.000
Arkansas	25.6412	3.2496	7.89	0.000
Arizona	26.6339	3.2277	8.25	0.000
California	26.5480	3.2434	8.19	0.000
Colorado	26.1724	3.2608	8.03	0.000
Connecticut	25.3270	3.2578	8.08	0.000
District of Columbia	26.0314	3.2699	7.96	0.000
Delaware	26.0525	3.2719	7.96	0.000
Florida	26.7896	3.2194	8.32	0.000
Georgia	26.4536	3.2545	8.13	0.000
Hawaii	23.8933	3.2676	7.31	0.000
Iowa	26.1666	3.2669	8.01	0.000
Idaho	25.3286	3.2630	7.76	0.000
Illinois	26.5186	3.2569	8.14	0.000
Indiana	26.3159	3.2619	8.07	0.000
Kansas	25.6968	3.2630	7.88	0.000
Kentucky	25.8271	3.2613	7.92	0.000
Louisiana	26.3165	3.2548	8.09	0.000
Massachusetts	26.4245	3.2557	8.12	0.000
Maryland	26.4151	3.2614	8.10	0.000
Maine	25.0056	3.2684	7.65	0.000
Michigan	26.2274	3.2515	8.07	0.000
Minnesota	26.3019	3.2628	8.06	0.000
Missouri	25.9973	3.2607	7.97	0.000
Mississippi	26.2978	3.2530	8.08	0.000
Montana	24.7679	3.2679	7.58	0.000
North Carolina	26.3227	3.2556	8.09	0.000
North Dakota	25.2256	3.2686	7.89	0.000
Nebraska	25.7297	3.2615	7.92	0.000
New Hampshire	25.8414	3.2635	7.92	0.000
New Jersey	26.3998	3.2477	8.13	0.000
New Mexico	26.1024	3.2650	7.99	0.000
Nevada	26.1382	3.2566	8.03	0.000
New York	26.2963	3.2417	8.11	0.000
Ohio	26.3468	3.2608	8.08	0.000
Oklahoma	25.8892	3.2644	7.93	0.000
Oregon	25.4513	3.2582	7.81	0.000
Pennsylvania	26.4789	3.2573	8.13	0.000
Rhode Island	25.1521	3.2683	8.00	0.000
South Carolina	26.4216	3.2433	8.15	0.000
South Dakota	25.4075	3.2665	7.78	0.000
Tennessee	26.0621	3.2686	8.02	0.000

Texas	26.8796	3.2213	8.34	0.000
Utah	25.7632	3.2536	7.92	0.000
Virginia	26.3402	3.2635	8.07	0.000
Vermont	24.3453	3.2683	7.45	0.000
Washington	26.0738	3.2581	8.00	0.000
Wisconsin	25.9419	3.2617	7.95	0.000
West Virginia	25.2368	3.2718	7.71	0.000
Wyoming	23.9943	3.2677	7.34	0.000
$LogDays_t$	-10.4430	1.5361	-6.80	0.000
$LogDays_t$*$LogDays_t$	1.1916	0.1799	6.30	0.000
$LogDailyDead_{it-7}$	0.8697	0.0246	35.32	0.000
$LogMaxTemp_{it-7}$	0.2988	0.0506	5.91	0.000
$LogMaxTemp_{it-14}$	0.3011	0.0545	5.52	0.000
R^2	0.9667			
Root MSE	9.3198			
Observations	4567			

Table A2. Model predicting NewPositives$_{it}$.

Variable	Coefficient	Robust S.E.	t-statistic	p-value
Alaska	44.3754	7.8220	5.67	0.000
Alabama	45.0719	7.7439	5.82	0.000
Arkansas	45.0296	7.7613	5.80	0.000
Arizona	45.4897	7.7481	5.87	0.000
California	45.2471	7.8135	5.79	0.000
Colorado	44.7237	7.7036	5.81	0.000
Connecticut	44.9710	7.8123	5.76	0.000
District of Columbia	44.8480	7.7886	5.76	0.000
Delaware	44.8834	7.7766	5.77	0.000
Florida	45.7236	7.8081	5.86	0.000
Georgia	45.2116	7.7504	5.83	0.000
Hawaii	43.5360	7.5748	5.75	0.000
Iowa	44.9210	7.7604	5.79	0.000
Idaho	44.4862	7.6268	5.83	0.000
Illinois	45.2043	7.8320	5.777	0.000
Indiana	44.7918	7.7378	5.79	0.000
Kansas	44.8676	7.6937	5.83	0.000
Kentucky	44.4355	7.7336	5.75	0.000
Louisiana	46.0003	7.9379	5.80	0.000
Massachusetts	45.0429	7.8516	5.74	0.000
Maryland	45.1639	7.8065	5.79	0.000
Maine	43.7347	7.6623	5.71	0.000
Michigan	44.6836	7.7889	5.74	0.000
Minnesota	44.8802	7.7795	5.77	0.000
Missouri	44.9420	7.7386	5.81	0.000
Mississippi	45.1696	7.7728	5.81	0.000
Montana	44.2548	7.6490	5.79	0.000
North Carolina	44.0362	7.549	5.81	0.000
North Dakota	44.4879	7.7784	5.72	0.000
Nebraska	44.8758	7.7590	5.78	0.000
New Hampshire	44.2714	7.7374	5.72	0.000
New Jersey	45.2459	7.8555	5.76	0.000
New Mexico	44.0833	7.8327	5.76	0.000
Nevada	45.1552	7.7471	5.83	0.000
New York	45.2907	7.8897	5.74	0.000
Ohio	44.6637	7.7159	5.79	0.000
Oklahoma	44.7409	7.7293	5.79	0.000
Oregon	43.9776	7.6495	5.75	0.000
Pennsylvania	44.8583	7.7437	5.79	0.000
Rhode Island	44.8480	7.8233	5.73	0.000
South Carolina	45.0818	7.7231	5.84	0.000
South Dakota	44.4405	7.7294	5.75	0.000
Tennessee	45.3233	7.8145	5.80	0.000

Texas	45.3508	7.7418	5.86	0.000
Utah	44.9916	7.7777	5.78	0.000
Virginia	45.0741	7.7745	5.80	0.000
Vermont	43.1094	7.6813	5.61	0.000
Washington	44.5409	7.7176	5.77	0.000
Wisconsin	44.7343	7.7540	5.77	0.000
West Virginia	44.1364	7.7090	5.73	0.000
Wyoming	43.7190	7.6626	5.71	0.000
$LogNewTests_{it}$	0.3855	0.0833	4.63	0.000
MONDAY	-0.0801	0.0329	-2.44	0.015
$LogDays_t$	-19.5476	3.7152	-5.62	0.000
$LogDays_t$*$LogDays_t$	2.3839	0.4551	5.24	0.000
$LogNewPositives_{it-7}$	0.5856	0.0469	12.48	0.000
$LogNewTests_{it-7}$	-0.1755	0.0584	-2.93	0.005
$PerCapitaTests_{it-7}$	-0.0096	0.0031	-3.13	0.002
$LogMaxTemp_{it-2}$	0.5435	0.1082	4.94	0.000
$LogMaxTemp_{it-7}$	0.6873	0.0460	14.94	0.000
R^2	0.9507			
Root MSE	303.503			
Observations	4592			

Table A3. Model predicting $StateBase_i$ taken from $DailyDead_{it}$ model.

Variable	Coefficient	Robust S.E.	t-statistic	p-value
Constant	-2.6082	0.2842	-9.18	0.000
LogPopulation	0.3652	0.0430	8.48	0.000
%Black	0.0197	0.0030	6.52	0.000
%Hispanic	0.0172	0.0049	3.54	0.001
%Age 80+	0.1163	0.0627	1.86	0.070
R^2	0.7938			
Root MSE	0.2845			
Observations	51			

Table A4. Alternative specifications for $DailyDead_{it}$ model. $StateIndicator_i$ for models provided in Table A6. Robust standard errors clustered at the state level.

Variable	**Eq. 1** Base Model	**Eq. 3** Linear MaxTemp	**Eq. 4** Ratio Scaler	**Eq. 5** Ratio Scaler Linear MaxTemp	**Eq. 6** 14^{th} Lag DailyDead	**Eq. 7** Rolling Weekly	**Eq. 12** Add UV
$LogDays_t$	-10.4430	-10.5842	-10.2210	-10.1283	-30.2125	-13.9640	-8.7000
	(1.5361)	(1.5407)	(1.5499)	(1.5545)	(2.3673)	(1.2216)	(1.3241)
$LogDays_t$*$LogDays_t$	1.1916	1.2093	1.1627	1.1524	3.4253	1.5895	1.0093
	(0.1799)	(0.1806)	(0.1810)	(0.1815)	(0.2850)	(0.1453)	(0.1565)
$LogDailyDead_{it-7}$	0.8697	0.8681	0.8738	0.8752			0.8585
	(0.0246)	(0.0248)	(0.0243)	(0.0243)			(0.0256)
$LogDailyDead_{it-14}$					0.8199		
					(0.0478)		
$LogWeeklyDead_{it-7}$						0.9280	
						(0.0373)	
$LogMaxTemp_{it-7}$	0.2988		-0.5907		0.1843		0.1364
	(0.0506)		(0.1019)		(0.1651)		(0.1326)
$LogMaxTemp_{it-14}$	0.3011		-0.5790		0.4681		0.2487
	(0.0545)		(0.0887)		(0.0726)		(0.0578)
$MaxTemp_{it-7}$		0.1131		-1.3414			
		(0.0190)		(0.2704)			
$MaxTemp_{it-14}$		0.1160		-1.3016			
		(0.0222)		(0.2224)			
$LogMaxTemp_{it-14}$						0.2215	
						(0.0454)	
$LogMaxTemp_{it-18}$						0.3292	
						(0.0523)	
							0.5213
							(0.2100)
							0.2962
							(0.1318)
R^2	0.9667	0.9667	0.9666	0.9666	0.9425	0.9903	0.9674
Root MSE	9.3198	9.3151	9.3322	9.3394	12.2483	37.8452	9.2235
Observations	4567	4567	4567	4567	4576	4552	4567

Table A5. AR(7) DailyDead$_{it}$ models using different Reported/Actual combinations. U.S. states: April 16-July 15. June 25 NJ death count (1877) set to missing in reported. (Robust standard errors clustered at state level).

	Eq. 18 Reported/Reported	**Eq. 19** Actual/Reported	**Eq. 20** Reported/Actual	**Eq. 21** Actual/Actual
DailyDead$_{it-7}$	0.6986	0.6681	0.7360	0.7854
	(0.0069)	(0.0067)	(0.0064)	(0.0035)
Constant	5.0046	6.6079	3.4596	3.1725
	(0.4210)	(0.4096)	(0.3862)	(0.2138)
R^2	0.6893	0.6820	0.7428	0.9148
RMSE	26.545	25.828	24.154	13.371
Observations	4639	4639	4639	4639

Table A6. Parameter estimates including state-level fixed effects for all models.

Model 1

Variable	Coefficient	S.E.
State_AK	24.2468	3.2668
State_AL	26.2830	3.2504
State_AR	25.6412	3.2496
State_AZ	26.6399	3.2277
State_CA	26.5480	3.2434
State_CO	26.1724	3.2608
State_CT	26.3270	3.2578
State_DC	26.0314	3.2699
State_DE	26.0525	3.2719
State_FL	26.7896	3.2194
State_GA	26.4536	3.2545
State_HI	23.8933	3.2676
State_IA	26.1666	3.2669
State_ID	25.3286	3.2630
State_IL	26.5186	3.2569
State_IN	26.3159	3.2619
State_KS	25.6968	3.2630
State_KY	25.8271	3.2613
State_LA	26.3165	3.2548
State_MA	26.4245	3.2557
State_MD	26.4151	3.2614
State_ME	25.0056	3.2684
State_MI	26.2274	3.2515
State_MN	26.3019	3.2628
State_MO	25.9973	3.2607
State_MS	26.2978	3.2530
State_MT	24.7679	3.2679
State_NC	26.3227	3.2556
State_ND	25.2256	3.2686
State_NE	25.7297	3.2615
State_NH	25.8414	3.2635
State_NJ	26.3998	3.2477
State_NM	26.1024	3.2650
State_NV	26.1382	3.2566
State_NY	26.2963	3.2417
State_OH	26.3468	3.2608
State_OK	25.8892	3.2644
State_OR	25.4513	3.2582
State_PA	26.4789	3.2573
State_RI	26.1521	3.2683
State_SC	26.4216	3.2433
State_SD	25.4075	3.2665
State_TN	26.0621	3.2486
State_TX	26.8796	3.2213
State_UT	25.7632	3.2536
State_VA	26.3402	3.2635
State_VT	24.3453	3.2683
State_WA	26.0738	3.2581
State_WI	25.9419	3.2617
State_WV	25.2368	3.2718
State_WY	23.9943	3.2677
t0	-10.4430	1.5361
t2	1.1916	0.1799
b1	0.8697	0.0246
w1	0.2988	0.0506
w2	0.3011	0.0545
R-square	0.9667	
Root MSE	9.3198	
Observations	4567	

Model 2

Variable	Coefficient	S.E.
LogPopulation	110.6656	5.0218
Good_Dates	-58.9392	10.3053
_cons	-799.2542	40.5126
R-square	0.0965	
Root MSE	330.1528	
Observations	4567	

Model 3

Variable	Coefficient	S.E.
State_AK	24.5529	3.2749
State_AL	26.6085	3.2602
State_AR	25.9674	3.2590
State_AZ	26.9905	3.2380
State_CA	26.8647	3.2529
State_CO	26.4937	3.2708
State_CT	26.6431	3.2674
State_DC	26.3474	3.2795
State_DE	26.3659	3.2813
State_FL	27.1275	3.2294
State_GA	26.7781	3.2646
State_HI	24.2219	3.2771
State_IA	26.4856	3.2764
State_ID	25.6418	3.2723
State_IL	26.8400	3.2668
State_IN	26.6345	3.2716
State_KS	26.0204	3.2729
State_KY	26.1429	3.2709
State_LA	26.6510	3.2655
State_MA	26.7435	3.2653
State_MD	26.7333	3.2713
State_ME	25.3192	3.2773
State_MI	26.5469	3.2613
State_MN	26.6185	3.2723
State_MO	26.3193	3.2706
State_MS	26.6264	3.2628
State_MT	25.0807	3.2770
State_NC	26.6467	3.2654
State_ND	25.5440	3.2777
State_NE	26.0525	3.2711
State_NH	26.1593	3.2730
State_NJ	26.7177	3.2579
State_NM	26.4317	3.2749
State_NV	26.4738	3.2667
State_NY	26.6136	3.2519
State_OH	26.6642	3.2703
State_OK	26.2148	3.2743
State_OR	25.7649	3.2675
State_PA	26.7961	3.2673
State_RI	26.4658	3.2776
State_SC	26.7494	3.2530
State_SD	25.7246	3.2758
State_TN	26.3870	3.2582
State_TX	27.2139	3.2313
State_UT	26.0825	3.2629
State_VA	26.6573	3.2733
State_VT	24.6667	3.2772
State_WA	26.3857	3.2676
State_WI	26.2584	3.2708
State_WV	25.5517	3.2811
State_WY	24.3020	3.2761
t0	-10.5842	1.5407
t2	1.2093	0.1806
b1	0.8681	0.0248
k1	0.1131	0.0190
k2	0.1160	0.0222
R-square	0.9667	
Root MSE	9.3152	
Observations	4567	

Model 4

Variable	Coefficient	S.E.
State_AK	20.1337	3.3174
State_AL	22.1346	3.2978
State_AR	21.4935	3.2976
State_AZ	22.4619	3.2750
State_CA	22.4087	3.2909
State_CO	22.0283	3.3069
State_CT	22.1941	3.3051
State_DC	21.8982	3.3169
State_DE	21.9243	3.3194
State_FL	22.6230	3.2668
State_GA	22.3049	3.3007
State_HI	19.7449	3.3147
State_IA	22.0278	3.3149
State_ID	21.2024	3.3106
State_IL	22.3739	3.3042
State_IN	22.1782	3.3090
State_KS	21.5547	3.3097
State_KY	21.6948	3.3089
State_LA	22.1540	3.2993
State_MA	22.2860	3.3037
State_MD	22.2768	3.3081
State_ME	20.8797	3.3174
State_MI	22.0856	3.2989
State_MN	22.1667	3.3107
State_MO	21.8541	3.3075
State_MS	22.1459	3.3003
State_MT	20.6421	3.3164
State_NC	22.1764	3.3026
State_ND	21.0901	3.3174
State_NE	21.5877	3.3092
State_NH	21.7067	3.3115
State_NJ	22.2613	3.2935
State_NM	21.9509	3.3120
State_NV	21.9790	3.3031
State_NY	22.1590	3.2876
State_OH	22.2103	3.3087
State_OK	21.7425	3.3109
State_OR	21.3224	3.3057
State_PA	22.3421	3.3038
State_RI	22.0239	3.3165
State_SC	22.2712	3.2909
State_SD	21.2743	3.3149
State_TN	21.9162	3.2961
State_TX	22.7186	3.2689
State_UT	21.6275	3.3019
State_VA	22.2043	3.3103
State_VT	20.2029	3.3185
State_WA	21.9464	3.3051
State_WI	21.8095	3.3107
State_WV	21.1075	3.3194
State_WY	19.8756	3.3181
t0	-10.2110	1.5499
t2	1.1627	0.1810
b1	0.8738	0.0243
a1	-0.5907	0.1019
a2	-0.5790	0.0887
R-square	0.9666	
Root MSE	9.3322	
Observations	4567	

Model 5

Variable	Coefficient	S.E.
State_AK	20.2699	3.3231
State_AL	22.2581	3.3039
State_AR	21.6173	3.3036
State_AZ	22.5749	3.2812
State_CA	22.5354	3.2970
State_CO	22.1544	3.3129
State_CT	22.3229	3.3110
State_DC	22.0268	3.3228
State_DE	22.0545	3.3253
State_FL	22.7402	3.2728
State_GA	22.4284	3.3067
State_HI	19.8683	3.3209
State_IA	22.1551	3.3209
State_ID	21.3334	3.3165
State_IL	22.4993	3.3102
State_IN	22.3055	3.3149
State_KS	21.6802	3.3157
State_KY	21.8238	3.3147
State_LA	22.2725	3.3055
State_MA	22.4136	3.3096
State_MD	22.4036	3.3140
State_ME	21.0117	3.3232
State_MI	22.2125	3.3050
State_MN	22.2947	3.3166
State_MO	21.9793	3.3134
State_MS	22.2682	3.3064
State_MT	20.7733	3.3223
State_NC	22.3006	3.3086
State_ND	21.2190	3.3233
State_NE	21.7133	3.3151
State_NH	21.8348	3.3174
State_NJ	22.3879	3.2995
State_NM	22.0732	3.3181
State_NV	22.0985	3.3093
State_NY	22.2860	3.2936
State_OH	22.3383	3.3147
State_OK	21.8670	3.3169
State_OR	21.4524	3.3116
State_PA	22.4694	3.3097
State_RI	22.1545	3.3224
State_SC	22.3941	3.2969
State_SD	21.4031	3.3208
State_TN	22.0405	3.3021
State_TX	22.8377	3.2749
State_UT	21.7553	3.3078
State_VA	22.3319	3.3163
State_VT	20.3324	3.3245
State_WA	22.0770	3.3110
State_WI	21.9391	3.3166
State_WV	21.2375	3.3253
State_WY	20.0103	3.3239
t0	-10.1283	1.5545
t2	1.1524	0.1815
b1	0.8752	0.0243
j1	-1.3414	0.2704
j2	-1.3016	0.2224
R-square	0.9666	
Root MSE	9.3394	
Observations	4567	

Model 6

Variable	Coefficient	S.E.
State_AK	68.0983	4.8708
State_AL	70.0627	4.8869
State_AR	69.3268	4.8655
State_AZ	70.5461	4.8661
State_CA	70.4218	4.9037
State_CO	69.8248	4.9467
State_CT	70.1264	4.9560
State_DC	69.8024	4.9293
State_DE	69.8608	4.9324
State_FL	70.6838	4.8716
State_GA	70.1762	4.9259
State_HI	67.5865	4.9040
State_IA	69.8836	4.9124
State_ID	68.7233	4.9201
State_IL	70.3744	4.9345
State_IN	70.0431	4.9376
State_KS	69.1838	4.9171
State_KY	69.5242	4.9171
State_LA	69.9121	4.9466
State_MA	70.3122	4.9548
State_MD	70.2614	4.9348
State_ME	68.7766	4.9195
State_MI	69.8819	4.9552
State_MN	70.0764	4.9105
State_MO	69.7402	4.9144
State_MS	70.1096	4.9029
State_MT	68.5028	4.8888
State_NC	70.0974	4.9015
State_ND	68.8297	4.9008
State_NE	69.3169	4.8851
State_NH	69.4363	4.8960
State_NJ	70.1194	4.9633
State_NM	69.8534	4.9026
State_NV	69.7741	4.9211
State_NY	69.9672	4.9672
State_OH	70.1541	4.9305
State_OK	69.5545	4.9309
State_OR	69.2116	4.9088
State_PA	70.3375	4.9543
State_RI	69.9466	4.9329
State_SC	70.1774	4.8797
State_SD	69.0783	4.8834
State_TN	69.6894	4.8964
State_TX	70.8674	4.8732
State_UT	69.4429	4.8863
State_VA	70.1628	4.9326
State_VT	67.8890	4.9203
State_WA	69.4145	4.9331
State_WI	69.4335	4.9177
State_WV	68.9390	4.9132
State_WY	67.3690	4.8829
t0	-30.2125	2.3673
t2	3.4253	0.2850
b1	0.8199	0.0478
d1	0.1843	0.1651
d2	0.4681	0.0726
R-square	0.9425	
Root MSE	12.2483	
Observations	4567	

Model 7

Variable	Coefficient	S.E.
State_AK	32.9102	2.6235
State_AL	34.0669	2.7254
State_AR	33.8438	2.6948
State_AZ	34.2783	2.7475
State_CA	34.1784	2.7625
State_CO	33.8629	2.7479
State_CT	33.9715	2.7669
State_DC	33.9732	2.7261
State_DE	33.9674	2.7253
State_FL	34.3485	2.7639
State_GA	34.1048	2.7569
State_HI	32.9555	2.6727
State_IA	34.0259	2.7253
State_ID	33.3378	2.6796
State_IL	34.1271	2.7718
State_IN	34.0090	2.7508
State_KS	33.7194	2.7060
State_KY	33.8415	2.7138
State_LA	33.9520	2.7729
State_MA	34.0373	2.7750
State_MD	34.0977	2.7607
State_ME	33.4256	2.6726
State_MI	33.8339	2.7745
State_MN	34.0356	2.7370
State_MO	33.9426	2.7337
State_MS	34.0962	2.7307
State_MT	33.4258	2.6469
State_NC	34.0766	2.7367
State_ND	33.6488	2.6754
State_NE	33.7940	2.6973
State_NH	33.8766	2.7025
State_NJ	33.9433	2.7998
State_NM	34.0438	2.7222
State_NV	33.9905	2.7232
State_NY	33.8453	2.8111
State_OH	34.0392	2.7488
State_OK	33.7927	2.7157
State_OR	33.7039	2.6892
State_PA	34.0933	2.7813
State_RI	33.9590	2.7275
State_SC	34.1241	2.7177
State_SD	33.6997	2.6770
State_TN	33.9789	2.7113
State_TX	34.4291	2.7524
State_UT	33.9061	2.6837
State_VA	34.0636	2.7508
State_VT	33.0951	2.6638
State_WA	33.7650	2.7259
State_WI	33.7719	2.7117
State_WV	33.6192	2.6880
State_WY	33.1590	2.6433
t0	-13.9640	1.2216
t2	1.5895	0.1453
b1	0.9280	0.0373
h1	0.2215	0.0454
h2	0.3292	0.0523
R-square	0.9903	
Root MSE	37.8452	
Observations	4552	

Model 8

Variable	Coefficient	S.E.
State_AK	35.3125	4.9526
State_AL	37.5093	5.0265
State_AR	39.9268	6.7158
State_AZ	37.7874	4.9858
State_CA	37.5128	4.9174
State_CO	37.2238	4.9732
State_CT	37.3223	4.9562
State_DC	37.1079	5.0228
State_DE	36.9748	4.9447
State_FL	38.0022	5.0012
State_GA	37.7061	5.0454
State_HI	34.8410	4.9367
State_IA	40.4395	6.6952
State_ID	36.2677	4.9392
State_IL	37.5012	4.9429
State_IN	37.3513	4.9613
State_KS	36.7697	4.9970
State_KY	36.8543	4.9687
State_LA	37.2923	4.9540
State_MA	37.4709	4.9703
State_MD	37.5591	5.0236
State_ME	36.1441	5.0254
State_MI	37.2267	4.9576
State_MN	37.3694	4.9796
State_MO	37.2742	5.0676
State_MS	37.4815	5.0134
State_MT	35.7994	4.9576
State_NC	37.4502	5.0010
State_ND	39.5098	6.7049
State_NE	40.0185	6.7035
State_NH	36.8973	4.9704
State_NJ	37.3833	4.9410
State_NM	37.0723	4.9427
State_NV	37.2553	5.0116
State_NY	37.3281	4.9554
State_OH	37.3592	4.9516
State_OK	39.8591	6.5531
State_OR	36.3622	4.9248
State_PA	37.7060	5.0665
State_RI	37.2153	4.9853
State_SC	37.6689	5.0245
State_SD	39.7644	6.7388
State_TN	37.2144	4.9961
State_TX	38.0718	4.9929
State_UT	39.8857	6.6641
State_VA	37.4447	5.0106
State_VT	35.2688	4.9384
State_WA	36.9972	4.9326
State_WI	36.9340	4.9507
State_WV	36.1957	4.9344
State_WY	38.3688	6.7926
t0	-15.8165	2.4326
t2	1.6788	0.2216
s1	0.8278	0.5701
s2	-0.0520	0.0253
b1	0.8318	0.0247
w1	0.2903	0.0482
w2	0.2849	0.0495
R-square	0.9677	
Root MSE	9.1764	
Observations	4567	

Model 9

Variable	Coefficient	S.E.
State_AK	1.8320	0.3592
State_AL	3.6712	0.4368
State_AR	2.3075	0.1980
State_AZ	4.0871	0.5048
State_CA	3.9824	0.5123
State_CO	3.6027	0.4206
State_CT	3.7619	0.4606
State_DC	3.5902	0.3880
State_DE	3.6529	0.4065
State_FL	4.1604	0.5430
State_GA	3.7659	0.4377
State_HI	1.5444	0.3470
State_IA	2.7473	0.1963
State_ID	2.9995	0.3601
State_IL	3.9148	0.5004
State_IN	3.7293	0.4461
State_KS	3.2786	0.3736
State_KY	3.3538	0.4161
State_LA	3.7792	0.4412
State_MA	3.7945	0.4852
State_MD	3.8027	0.4474
State_ME	2.6020	0.3471
State_MI	3.6610	0.4664
State_MN	3.7560	0.4508
State_MO	3.3604	0.4222
State_MS	3.7118	0.4328
State_MT	2.3461	0.3493
State_NC	3.7650	0.4384
State_ND	1.9761	0.1599
State_NE	2.3871	0.1875
State_NH	3.3717	0.4212
State_NJ	3.7457	0.5071
State_NM	3.6508	0.4188
State_NV	3.6601	0.3946
State_NY	3.5950	0.5251
State_OH	3.7773	0.4583
State_OK	2.5978	0.1798
State_OR	3.1231	0.3872
State_PA	3.7882	0.4607
State_RI	3.6310	0.4157
State_SC	3.8521	0.4282
State_SD	2.0854	0.1686
State_TN	3.5423	0.4293
State_TX	4.2796	0.5281
State_UT	2.5229	0.1775
State_VA	3.7735	0.4327
State_VT	2.1092	0.3380
State_WA	3.6787	0.4133
State_WI	3.5068	0.4234
State_WV	2.8448	0.3730
State_WY	0.8432	0.1415
s1	-0.2059	0.0909
s2	0.0703	0.0183
b1	0.9662	0.0441
w1	0.2678	0.0544
w2	0.2130	0.0771
R-square	0.9622	
Root MSE	9.9251	
Observations	4567	

Model 10

Variable	Coefficient	S.E.
State_AK	26.8779	3.2441
State_AL	28.9128	3.2286
State_AR	28.2708	3.2280
State_AZ	29.2751	3.2005
State_CA	29.1775	3.2217
State_CO	28.8056	3.2357
State_CT	28.9574	3.2353
State_DC	28.6617	3.2477
State_DE	28.6829	3.2497
State_FL	29.4184	3.1982
State_GA	29.0838	3.2322
State_HI	26.5230	3.2463
State_IA	28.7965	3.2449
State_ID	27.9617	3.2382
State_IL	29.1492	3.2343
State_IN	28.9459	3.2399
State_KS	28.3278	3.2402
State_KY	28.4573	3.2392
State_LA	28.9455	3.2337
State_MA	29.0544	3.2337
State_MD	29.0454	3.2391
State_ME	27.6359	3.2462
State_MI	28.8579	3.2290
State_MN	28.9328	3.2397
State_MO	28.6276	3.2382
State_MS	28.9273	3.2314
State_MT	27.4010	3.2435
State_NC	28.9526	3.2336
State_ND	27.8562	3.2459
State_NE	28.3603	3.2390
State_NH	28.4725	3.2400
State_NJ	29.0300	3.2255
State_NM	28.7391	3.2366
State_NV	28.7745	3.2286
State_NY	28.9253	3.2207
State_OH	28.9768	3.2388
State_OK	28.5192	3.2425
State_OR	28.0822	3.2355
State_PA	29.1095	3.2347
State_RI	28.7823	3.2463
State_SC	29.0509	3.2219
State_SD	28.0382	3.2439
State_TN	28.6923	3.2264
State_TX	29.5088	3.1998
State_UT	28.3967	3.2283
State_VA	28.9706	3.2412
State_VT	26.9756	3.2467
State_WA	28.7046	3.2355
State_WI	28.5722	3.2397
State_WV	27.8668	3.2499
State_WY	26.6265	3.2436
t0	-10.4435	1.5277
t2	1.1916	0.1790
b1	0.8698	0.0246
w1	0.3033	0.0680
w2	0.3054	0.0696
a1	-0.0079	0.0469
a2	-0.0087	0.0460
R-square	0.9667	
Root MSE	9.3217	
Observations	4567	

Model 11

Variable	Coefficient	S.E.
State_AK	26.9609	3.3219
State_AL	28.9971	3.3067
State_AR	28.3566	3.3060
State_AZ	29.3271	3.2730
State_CA	29.2619	3.2998
State_CO	28.8851	3.3155
State_CT	29.0422	3.3141
State_DC	28.7447	3.3246
State_DE	28.7667	3.3274
State_FL	29.5033	3.2764
State_GA	29.1664	3.3097
State_HI	26.6045	3.3212
State_IA	28.8814	3.3228
State_ID	28.0400	3.3156
State_IL	29.2323	3.3130
State_IN	29.0312	3.3180
State_KS	28.4099	3.3172
State_KY	28.5421	3.3170
State_LA	29.0298	3.3095
State_MA	29.1391	3.3117
State_MD	29.1288	3.3173
State_ME	27.7199	3.3232
State_MI	28.9423	3.3073
State_MN	29.0141	3.3178
State_MO	28.7101	3.3157
State_MS	29.0130	3.3094
State_MT	27.4784	3.3209
State_NC	29.0372	3.3116
State_ND	27.9402	3.3240
State_NE	28.4443	3.3174
State_NH	28.5546	3.3183
State_NJ	29.1130	3.3032
State_NM	28.7988	3.3131
State_NV	28.8261	3.2988
State_NY	29.0122	3.2984
State_OH	29.0620	3.3170
State_OK	28.6046	3.3198
State_OR	28.1656	3.3131
State_PA	29.1915	3.3127
State_RI	28.8678	3.3245
State_SC	29.1369	3.3002
State_SD	28.1215	3.3218
State_TN	28.7762	3.3044
State_TX	29.5947	3.2791
State_UT	28.4689	3.3040
State_VA	29.0544	3.3193
State_VT	27.0602	3.3232
State_WA	28.7882	3.3135
State_WI	28.6559	3.3170
State_WV	27.9526	3.3273
State_WY	26.7093	3.3234
t0	-10.4301	1.5426
t2	1.1901	0.1809
b1	0.8696	0.0248
w1	0.2950	0.0568
w2	0.2997	0.0579
a1	0.0571	0.1556
a2	0.0489	0.1600
R-square	0.9667	
Root MSE	9.3210	
Observations	4567	

Model 12

Variable	Coefficient	S.E.
State_AK	22.6847	2.8044
State_AL	25.1718	2.7852
State_AR	24.5079	2.7841
State_AZ	25.5209	2.7633
State_CA	25.4578	2.7795
State_CO	25.0437	2.7958
State_CT	25.1276	2.7915
State_DC	24.8483	2.8024
State_DE	24.8631	2.8045
State_FL	25.7442	2.7570
State_GA	25.3558	2.7893
State_HI	22.8186	2.8026
State_IA	24.9829	2.7995
State_ID	24.0953	2.7966
State_IL	25.3361	2.7902
State_IN	25.1426	2.7954
State_KS	24.5349	2.7971
State_KY	24.6568	2.7946
State_LA	25.2766	2.7917
State_MA	25.2375	2.7903
State_MD	25.2423	2.7944
State_ME	23.7763	2.8028
State_MI	25.0237	2.7851
State_MN	25.0833	2.7955
State_MO	24.8275	2.7937
State_MS	25.1949	2.7877
State_MT	23.5121	2.8019
State_NC	25.1977	2.7895
State_ND	23.9670	2.8017
State_NE	24.5407	2.7947
State_NH	24.6115	2.7965
State_NJ	25.2245	2.7820
State_NM	25.0030	2.7989
State_NV	24.9894	2.7899
State_NY	25.1382	2.7770
State_OH	25.1625	2.7942
State_OK	24.7573	2.7998
State_OR	24.1740	2.7918
State_PA	25.3055	2.7906
State_RI	24.9457	2.8015
State_SC	25.3066	2.7785
State_SD	24.1938	2.7990
State_TN	24.9281	2.7831
State_TX	25.7912	2.7588
State_UT	24.6060	2.7886
State_VA	25.1686	2.7964
State_VT	23.1031	2.8024
State_WA	24.7820	2.7913
State_WI	24.7357	2.7956
State_WV	24.0587	2.8047
State_WY	22.8521	2.8023
t0	-8.7000	1.3241
t2	1.0093	0.1565
b1	0.8585	0.0256
w1	0.1364	0.1326
w2	0.2487	0.0578
a1	0.5213	0.2100
a2	0.2962	0.1318
R-square	0.9674	
Root MSE	9.2236	
Observations	4567	

Model 13

Variable	Coefficien	S.E.
State_AK	16.9355	3.469
State_AL	19.5465	3.481
State_AR	18.8769	3.478
State_AZ	19.8707	3.459
State_CA	19.8457	3.474
State_CO	19.4279	3.485
State_CT	19.4921	3.473
State_DC	19.2066	3.491
State_DE	19.2292	3.492
State_FL	20.1358	3.454
State_GA	19.7321	3.484
State_HI	17.2231	3.502
State_IA	19.3406	3.489
State_ID	18.4468	3.480
State_IL	19.6902	3.477
State_IN	19.5082	3.483
State_KS	18.8991	3.487
State_KY	19.0255	3.482
State_LA	19.6669	3.491
State_MA	19.6161	3.471
State_MD	19.5957	3.483
State_ME	18.1559	3.483
State_MI	19.3781	3.464
State_MN	19.4252	3.482
State_MO	19.1811	3.484
State_MS	19.5727	3.485
State_MT	17.8518	3.486
State_NC	19.5672	3.484
State_ND	18.3113	3.486
State_NE	18.8928	3.485
State_NH	18.9573	3.483
State_NJ	19.5782	3.464
State_NM	19.3860	3.498
State_NV	19.3380	3.483
State_NY	19.5042	3.457
State_OH	19.5297	3.480
State_OK	19.1450	3.492
State_OR	18.4967	3.472
State_PA	19.6612	3.476
State_RI	19.3154	3.486
State_SC	19.6827	3.473
State_SD	18.5425	3.487
State_TN	19.2969	3.475
State_TX	20.1672	3.453
State_UT	18.9864	3.480
State_VA	19.5268	3.485
State_VT	17.4780	3.481
State_WA	19.0949	3.470
State_WI	19.1108	3.479
State_WV	18.4304	3.494
State_WY	17.2778	3.492
t0	-7.4256	1.630
t2	0.8685	0.191
b1	0.8611	0.026
a1	0.6316	0.119
a2	0.4650	0.075
R-square	0.9669	
Root MSE	9.2939	
Observation	4567	

Model 14

Variable	Coefficien	S.E.
State_AK	9.5460	9.9804
State_AL	11.9991	9.6295
State_AR	11.1770	9.7777
State_AZ	12.4550	9.5622
State_CA	12.2251	9.6924
State_CO	12.1578	9.4485
State_CT	12.6507	9.2511
State_DC	12.1266	9.3667
State_DE	12.0615	9.4223
State_FL	12.6138	9.5721
State_GA	12.3328	9.5209
State_HI	9.0987	10.0746
State_IA	11.8945	9.6341
State_ID	10.9464	9.7317
State_IL	12.4810	9.4842
State_IN	12.2584	9.4792
State_KS	11.3863	9.6608
State_KY	11.5100	9.6686
State_LA	12.5174	9.3058
State_MA	12.6781	9.3068
State_MD	12.3900	9.4628
State_ME	10.6601	9.6958
State_MI	12.4468	9.3113
State_MN	12.0540	9.6219
State_MO	11.6962	9.6647
State_MS	12.1683	9.5118
State_MT	10.0719	9.9861
State_NC	11.9679	9.7043
State_ND	10.8321	9.7155
State_NE	11.3572	9.7069
State_NH	11.6095	9.5981
State_NJ	12.9440	9.1431
State_NM	11.8357	9.6202
State_NV	11.9364	9.5677
State_NY	12.7671	9.1862
State_OH	12.1716	9.5718
State_OK	11.5981	9.6537
State_OR	10.9724	9.8202
State_PA	12.5207	9.4291
State_RI	12.2865	9.3524
State_SC	12.1198	9.6376
State_SD	10.9780	9.7599
State_TN	11.6459	9.7493
State_TX	12.5037	9.7180
State_UT	11.2319	9.8406
State_VA	12.1622	9.5705
State_VT	10.0472	9.5578
State_WA	11.9331	9.5323
State_WI	11.6491	9.6614
State_WV	10.7205	9.8812
State_WY	9.3713	9.9413
t0	-4.5443	3.9531
t2	0.5808	0.4116
c1	-0.5533	0.3046
c2	0.0326	0.0347
b1	0.8778	0.0274
w1	0.2925	0.0515
w2	0.2981	0.0458
R-square	0.9679	
RMSE	9.1536	
Observatio	4567	

Model 15

Variable	Coefficien	S.E
State_AK	3.5952	8.7
State_AL	5.8859	8.4
State_AR	5.0183	8.5
State_AZ	6.3802	8.4
State_CA	6.0203	8.5
State_CO	6.1577	8.2
State_CT	6.8051	8.1
State_DC	6.2628	8.2
State_DE	6.1560	8.2
State_FL	6.4954	8.4
State_GA	6.2742	8.3
State_HI	3.1812	8.8
State_IA	5.8288	8.4
State_ID	4.8809	8.5
State_IL	6.4442	8.3
State_IN	6.2457	8.3
State_KS	5.2980	8.4
State_KY	5.3820	8.4
State_LA	6.6533	8.1
State_MA	6.7704	8.1
State_MD	6.3927	8.3
State_ME	4.5793	8.5
State_MI	6.5401	8.1
State_MN	5.9745	8.4
State_MO	5.5684	8.4
State_MS	6.1664	8.3
State_MT	4.0863	8.7
State_NC	5.8276	8.5
State_ND	4.7759	8.5
State_NE	5.2583	8.5
State_NH	5.5735	8.4
State_NJ	7.0991	8.0
State_NM	5.8012	8.4
State_NV	5.8771	8.4
State_NY	6.8951	8.0
State_OH	6.0791	8.4
State_OK	5.4982	8.4
State_OR	4.8834	8.6
State_PA	6.5106	8.2
State_RI	6.4248	8.2
State_SC	6.0074	8.4
State_SD	4.8780	8.5
State_TN	5.4874	8.5
State_TX	6.2748	8.5
State_UT	5.1468	8.6
State_VA	6.0770	8.4
State_VT	3.9987	8.3
State_WA	5.8807	8.3
State_WI	5.5418	8.4
State_WV	4.6024	8.6
State_WY	3.3305	8.6
t0	-2.4685	3.3
t2	0.3694	0.3
c1	-0.5198	0.2
c2	-0.0379	0.1
c3	-0.0058	0.0
c4	-0.0017	0.0
b1	0.9300	0.0
w1	0.2836	0.0
w2	0.2764	0.0
R-square	0.9691	
RMSE	8.9888	
Observations	4567	

Model 16

Variable	Coefficien	S.E.
State_AK	17.0018	5.543
State_AL	18.7653	5.641
State_AR	17.7498	5.625
State_AZ	19.7100	5.603
State_CA	19.9473	5.569
State_CO	19.3527	5.685
State_CT	19.6768	5.632
State_DC	18.4803	5.665
State_DE	18.4964	5.664
State_FL	20.3097	5.558
State_GA	19.4903	5.624
State_HI	17.0232	5.663
State_IA	18.5713	5.661
State_ID	17.5102	5.660
State_IL	19.9904	5.622
State_IN	19.6328	5.666
State_KS	17.9009	5.678
State_KY	18.5673	5.670
State_LA	18.8248	5.563
State_MA	19.8956	5.587
State_MD	19.4440	5.640
State_ME	17.9484	5.674
State_MI	20.1710	5.625
State_MN	19.2714	5.640
State_MO	19.0063	5.619
State_MS	18.8587	5.626
State_MT	17.7958	5.606
State_NC	19.1364	5.612
State_ND	17.2322	5.626
State_NE	17.7791	5.673
State_NH	18.6044	5.691
State_NJ	20.1089	5.617
State_NM	18.6012	5.609
State_NV	18.5251	5.616
State_NY	20.0549	5.555
State_OH	19.7788	5.660
State_OK	17.6217	5.667
State_OR	17.9494	5.662
State_PA	20.2618	5.644
State_RI	18.5871	5.607
State_SC	18.9771	5.617
State_SD	17.2530	5.674
State_TN	18.2918	5.584
State_TX	20.2237	5.597
State_UT	17.5312	5.598
State_VA	19.2248	5.646
State_VT	17.3072	5.641
State_WA	18.8195	5.607
State_WI	18.6382	5.628
State_WV	17.7771	5.633
State_WY	15.9743	5.677
t0	-6.8242	2.693
t2	0.5852	0.317
n1	-0.3077	0.084
pc1	0.5128	0.243
bp	0.7638	0.055
d3	0.2386	0.058
R-square	0.9406	
Root MSE	12.4556	
Observations	4567	

Model 17

Variable	Coefficien	S.E.
State_AK	44.3754	7.8
State_AL	45.0719	7.7
State_AR	45.0296	7.7
State_AZ	45.4897	7.7
State_CA	45.2471	7.8
State_CO	44.7237	7.7
State_CT	44.9710	7.8
State_DC	44.8480	7.7
State_DE	44.8834	7.7
State_FL	45.7236	7.8
State_GA	45.2116	7.7
State_HI	43.5360	7.5
State_IA	44.9209	7.7
State_ID	44.4862	7.6
State_IL	45.2043	7.8
State_IN	44.7918	7.7
State_KS	44.8676	7.6
State_KY	44.4355	7.7
State_LA	46.0003	7.9
State_MA	45.0429	7.8
State_MD	45.1639	7.8
State_ME	43.7347	7.6
State_MI	44.6835	7.7
State_MN	44.8802	7.7
State_MO	44.9420	7.7
State_MS	45.1696	7.7
State_MT	44.2548	7.6
State_NC	45.0362	7.7
State_ND	44.4879	7.7
State_NE	44.8758	7.7
State_NH	44.2717	7.7
State_NJ	45.2459	7.8
State_NM	45.0833	7.8
State_NV	45.1552	7.7
State_NY	45.2907	7.8
State_OH	44.6637	7.7
State_OK	44.7409	7.7
State_OR	43.9776	7.6
State_PA	44.8583	7.7
State_RI	44.8480	7.8
State_SC	45.0818	7.7
State_SD	44.4404	7.7
State_TN	45.3233	7.8
State_TX	45.3508	7.7
State_UT	44.9916	7.7
State_VA	45.0741	7.7
State_VT	43.1094	7.6
State_WA	44.5409	7.7
State_WI	44.7343	7.7
State_WV	44.1364	7.7
State_WY	43.7190	7.6
nt0	0.3855	0.0
mt	-0.0801	0.0
t1	-19.5476	3.7
t2	2.3839	0.4
nt7	-0.1655	0.0
b1	0.5856	0.0
pc1	-0.0096	0.0
w1	0.5435	0.1
w2	0.6873	0.0
R-square	0.9507	
Root MSE	303.5030	
Observatio	4592	

Model 18

Variable	Coefficien	S.E.
L7.ReportedDailyD	0.6986	0.006
_cons	5.0046	0.421
R-square	0.6893	
Root MSE	26.5453	
Observations	4639	

Model 19

Variable	Coefficien	S.E.
L7.ReportedDailyD	0.6681	0.006
_cons	6.6079	0.409
R-square	0.6820	
Root MSE	25.8280	
Observations	4639	

Model 20

Variable	Coefficien	S.E.
L7.DailyDead	0.7360	0.006
_cons	3.4596	0.386
R-square	0.7428	
Root MSE	24.1541	
Observations	4639	

Model 21

Variable	Coefficien	S.E.
L7.DailyDead	0.7854	0.003
_cons	3.1725	0.213
R-square	0.9148	
Root MSE	13.3709	
Observations	4639	

Model 22

Variable	Coefficient
State_AK	0.2006
State_AL	1.5370
State_AR	0.8090
State_AZ	2.1963
State_CA	2.0034
State_CO	1.3761
State_CT	1.6062
State_DC	1.1951
State_DE	1.2206
State_FL	2.5509
State_GA	1.8229
State_HI	0.1409
State_IA	1.3681
State_ID	0.5918
State_IL	1.9454
State_IN	1.5884
State_KS	0.8553
State_KY	0.9743
State_LA	1.5894
State_MA	1.7707
State_MD	1.7541
State_ME	0.4285
State_MI	1.4539
State_MN	1.5664
State_MO	1.1551
State_MS	1.5599
State_MT	0.3378
State_NC	1.5993
State_ND	0.5339
State_NE	0.8839
State_NH	0.9883
State_NJ	1.7275
State_NM	1.2831
State_NV	1.3298
State_NY	1.5576
State_OH	1.6383
State_OK	1.0367
State_OR	0.6691
State_PA	1.8697
State_RI	1.3484
State_SC	1.7655
State_SD	0.6404
State_TN	1.2324
State_TX	2.7912
State_UT	0.9140
State_VA	1.6275
State_VT	0.2214
State_WA	1.2469
State_WI	1.0928
State_WV	0.5399
State_WY	0.1559

Model 23

Variable	Coefficient	S.E.
LogPopulatio	0.3652	0.0430
PercentBlack	0.0197	0.0030
PercentHispa	0.0172	0.0049
PercentAge8	0.1163	0.0627
_cons	-2.6082	0.2842
R-square	0.7938	
Root MSE	0.2845	
Observations	51	

Model 24

Variable	Coefficient
State_AK	30.8645
State_AL	236.4667
State_AR	124.4626
State_AZ	337.8853
State_CA	308.2178
State_CO	211.7076
State_CT	247.1032
State_DC	183.8660
State_DE	187.7866
State_FL	392.4490
State_GA	280.4530
State_HI	21.6738
State_IA	210.4832
State_ID	91.0498
State_IL	299.2881
State_IN	244.3758
State_KS	131.5789
State_KY	149.8908
State_LA	244.5222
State_MA	272.4093
State_MD	269.8608
State_ME	65.9177
State_MI	223.6777
State_MN	240.9784
State_MO	177.7016
State_MS	239.9922
State_MT	51.9721
State_NC	246.0431
State_ND	82.1384
State_NE	135.9798
State_NH	152.0495
State_NJ	265.7632
State_NM	197.3949
State_NV	204.5898
State_NY	239.6327
State_OH	252.0446
State_OK	159.4940
State_OR	102.9358
State_PA	287.6393
State_RI	207.4532
State_SC	271.6207
State_SD	98.5245
State_TN	189.5980
State_TX	429.4077
State_UT	140.6124
State_VA	250.3867
State_VT	34.0594
State_WA	191.8292
State_WI	168.1248
State_WV	83.0635
State_WY	23.9773

Model 25

Variable	Coefficient
State_AK	0.1660
State_AL	1.2716
State_AR	0.6693
State_AZ	1.8169
State_CA	1.6574
State_CO	1.1384
State_CT	1.3288
State_DC	0.9887
State_DE	1.0098
State_FL	2.1103
State_GA	1.5081
State_HI	0.1165
State_IA	1.1318
State_ID	0.4896
State_IL	1.6094
State_IN	1.3141
State_KS	0.7075
State_KY	0.8060
State_LA	1.3149
State_MA	1.4648
State_MD	1.4511
State_ME	0.3545
State_MI	1.2028
State_MN	1.2958
State_MO	0.9556
State_MS	1.2905
State_MT	0.2795
State_NC	1.3231
State_ND	0.4417
State_NE	0.7312
State_NH	0.8176
State_NJ	1.4291
State_NM	1.0615
State_NV	1.1001
State_NY	1.2886
State_OH	1.3553
State_OK	0.8577
State_OR	0.5535
State_PA	1.5467
State_RI	1.1155
State_SC	1.4606
State_SD	0.5298
State_TN	1.0195
State_TX	2.3091
State_UT	0.7561
State_VA	1.3464
State_VT	0.1831
State_WA	1.0315
State_WI	0.9041
State_WV	0.4467
State_WY	0.1289

Model 26

Variable	Coefficient	S.E.
State_AK	19.1718	5.5455
State_AL	22.8740	5.5486
State_AR	22.0474	5.5568
State_AZ	23.5269	5.5377
State_CA	23.6248	5.5105
State_CO	22.8014	5.5331
State_CT	23.1423	5.5123
State_DC	22.3685	5.5664
State_DE	22.3263	5.5622
State_FL	23.5596	5.5434
State_GA	23.2117	5.5427
State_HI	19.7769	5.6115
State_IA	22.5782	5.5493
State_ID	20.8793	5.5795
State_IL	23.5277	5.5071
State_IN	23.0678	5.5314
State_KS	21.8978	5.5721
State_KY	22.2463	5.5515
State_LA	23.1644	5.5624
State_MA	23.3854	5.4903
State_MD	23.1839	5.5355
State_ME	21.1217	5.5520
State_MI	23.1641	5.5079
State_MN	22.9096	5.5305
State_MO	22.6315	5.5517
State_MS	22.8856	5.5500
State_MT	20.5095	5.5764
State_NC	23.0000	5.5447
State_ND	21.0049	5.5624
State_NE	21.9977	5.5622
State_NH	22.1678	5.5486
State_NJ	23.7615	5.5012
State_NM	22.4717	5.5759
State_NV	22.4211	5.5878
State_NY	23.7318	5.4834
State_OH	23.1541	5.5151
State_OK	22.1275	5.5729
State_OR	21.6158	5.5637
State_PA	23.4885	5.5143
State_RI	22.5008	5.5332
State_SC	22.7793	5.5456
State_SD	21.4924	5.5670
State_TN	22.5039	5.5482
State_TX	23.4079	5.5367
State_UT	21.9073	5.5616
State_VA	22.9497	5.5357
State_VT	20.5659	5.5622
State_WA	22.4466	5.5406
State_WI	22.2606	5.5282
State_WV	21.2802	5.5830
State_WY	19.8045	5.5516
t0	-7.7761	2.6721
t2	0.8279	0.3255
b1	0.5529	0.0634
w1	0.3298	0.0830
w2	0.5021	0.0666
R-square	0.8082	
Root MSE	22.9496	
Observations	4565	

Additional References

24. E. C. Schneider, Failing the test—the tragic data gap undermining the US pandemic response. *N. Engl. J. Med.* **383**, 299-302. doi: 10.1056/NEJMp2014836 (2020).

25. M. Salerno, F. Sessa, A. Piscopo, A. Montana, M. Torrisi, F. Patanè, P. Murabito, G. L. Volti, C. Pomara, No autopsies on COVID-19 deaths: a missed opportunity and the lockdown of science. *J. Clin. Med.* **9**, 1472 (2020).

26. D.M. Weinberger, J. Chen, T. Cohen, F.W. Crawford, F. Mostashari, D. Olson, V.E. Pitzer, N.G. Reich, M. Russi, L. Simonsen, A. Watkins, Estimation of excess deaths associated with the COVID-19 pandemic in the United States, March to May 2020. *JAMA Intern. Med.,* doi:10.1001/jamainternmed. 2020 .3391 Publishe (2020).

26. U.S. Center for Disease Control. Planning scenarios. https://www.cdc.gov/coronavirus/2019-ncov/hcp/planning-scenarios.html, retrieved 30 June 2020.

28. C. Courtemanche, J. Garuccio, A. Le, J. Pinkston, A. Yelowitz, Strong social distancing measures in the United States reduced the COVID-19 growth rate: study evaluates the impact of social distancing measures on the growth rate of confirmed COVID-19 cases across the United States. *Health Affairs* **10**, 1377 (2020).

29. A. Goolsbee, N. B. Luo, R. Nesbitt, C. Syverson, Lockdown Policies at the State and Local Level. doi: http://dx.doi.org/10.2139/ssrn.3682144 (20 Aug 2020).

30. R. Chetty, J. N. Friedman, N. Hendren, M. Stepner, How did covid-19 and stabilization policies affect spending and employment? a new real-time economic tracker based on private sector data. doi: http://dx.doi.org/10.3386/w27431 (25 June 2020).